Nanoscale Engineering for Reducing Phase Noise in Electronic Devices

PETER H. HANDEL, SENIOR MEMBER, IEEE, AND ADAM G. TOURNIER

Invited Paper

An investigation of electronic $1/f$ noise in ultrasmall devices and systems is presented, focused on nanoscale engineering of electronic devices for low phase noise. The investigation is based on the quantum $1/f$ formulas. Nanotechnology raises new questions of electronic noise, since fluctuations are more important in smaller devices. Based on the quantum $1/f$ noise theory, we find that in a certain transition range of sizes this general law is suspended, but reappears for $1/f$ noise in the nanometer domain, where the transition from coherent to conventional quantum $1/f$ effect is complete. The coherent and conventional quantum $1/f$ effects and their connection are briefly derived. The resulting quantum $1/f$ formulas are used to derive the $1/f$ noise of GaN/AlGaN MODFETs, resonant tunneling diodes, bulk acoustic wave and surface acoustic wave quartz resonators, microelectromechanical systems resonators, and spin valves. They are also used to calculate phase noise in these devices and in oscillators based on them, from first principles along with some classical noise sources. Device optimization is thus facilitated for ultrasmall devices.

Keywords*—*GaN/AlGaN MODFET oscillator phase noise, microelectromechanical devices, microresonators, nanosensors, nanotechnology, phase noise, quantum $1/f$ phase noise, quantum $1/f$ theory, spintronic $1/f$ noise, $1/f$ noise.

I. INTRODUCTION

The sensitivity of electronic systems is fundamentally limited by electronic noise [1], which places a lower limit on the signal-to-noise ratio that can be detected. Although it is possible to use correlation techniques to detect signals below the noise floor in certain applications, noise is the fundamental limitation to system sensitivity. Phase noise [2]–[5] presents a major obstacle for direct detection systems and makes more complicated heterodyne systems necessary for many applications.

Noise is an ensemble phenomenon and is characterized by the statistics of large numbers of electrons and their fluctuations. The derivations of conventional and coherent quantum $1/f$ noise in Section II show a general $1/N$ dependence of the power spectral density of $1/f$ noise in both cases. Here N is the number of current carriers used to define the electric current. Advances in nanotechnology produce opportunities to investigate noise performance, based on reduced number of electrons. The small number of electrons associated with these nanostructures forces a rethinking of the very concept of noise, with implications for system development and operation. Indeed, the surprising and fascinating result provided by the quantum $1/f$ noise theory is the presence of a transition between two related forms of fundamental $1/f$ noise, caused by the conventional and coherent quantum $1/f$ effect, respectively. Both forms are always part of the observed $1/f$ noise, but the former dominates in ultrasmall electronic devices, while the latter controls mainly devices with a large number of carriers, as shown in Section II-C.

Phase noise is important for military and civilian applications. The basic concepts are introduced in Section I-A below. Special emphasis was thus placed on quantum $1/f$ phase noise in RF and microwave devices, oscillators, and systems in general. Leeson's formula was modified by us radically for this purpose by the inclusion of a new quantum $1/f$ noise term proportional to the inverse fourth power of the quality factor. This is essential close to the carrier for all high-stability systems. The first principles derivation of the conventional and coherent quantum $1/f$ noise in Section II, is presented in elementary physical terms, easily accessible to engineers on an intuitive basis, sacrificing the rigor of second-quantized derivation in favor of increased transparency. There are no adjustable parameters or fudge factors in any of the derivations in this paper. Everything results from Maxwell's equations for the fields and Schrödinger's equation for the electrons. The same elementary physical approach is used to introduce the connection between the

Manuscript received March 4, 2005; revised May 4, 2005. This work was supported in part by the U.S. Army Research Office under Grant ARO W9911NF-04-1-0182, in part by the Ultralow Phase Noise MURI , in part by ONR, and in part by AFOSR.

P. H. Handel is with the Department of Physics and Astronomy and the Center for Molecular Electronics, University of Missouri, St. Louis, MO 63121 USA (e-mail: handel@umsl.edu).

A. G. Tournier is with the Department of Physics and Astronomy, University of Missouri, St. Louis, MO 63121 USA (e-mail: adamtournier@hotmail.com; adamtournier@umsl.edu).

Digital Object Identifier 10.1109/JPROC.2005.855451

coherent and conventional effect in Section II-D. Here special attention is given for the first time to the particular case of FETs and heterostructure FETs (HFETs) with widths w much larger than their length L_{DS}, e.g., by three orders of magnitude. This special geometry has obviously anticipated through trial and error the exact predictions of the quantum $1/f$ theory, which allows for decrease of $1/f$ noise with no transition to the much larger coherent quantum $1/f$ effect.

This paper derives in Section III simple formulas for the quantum $1/f$ noise of kinetic processes and dissipation rates in semiconductor nanodevices, quartz crystals, microelectromechanical systems (MEMS), and nanomechanical systems (NEMS). The quantum $1/f$ effect is shown to cause $1/f$ noise in devices such as GaN HFETs, resonant tunneling diodes (RTDs), MEMS resonators, spin valves, etc. These $1/f$ base-band contributions result in $1/f^3$ phase noise close to the carrier frequency.

Solid-state microwave generators of increased power can be obtained by using wide-bandgap materials, such as GaN and by coherently adding the output of many nanoscale devices. In Sections III-A and III-B, we have obtained from first principles an analytical formula for quantum $1/f$ noise in GaN/AlGaN HFETs that agrees with the experimental data (Section III-C), including also our own measurements. This allows optimization of the device and of the oscillating system based on it, as is shown in Section IV. We obtain a strong $1/f$ noise increase in the channel with gate voltage, even without gate leakage.

$1/f$ noise in bent ultrathin semiconductor samples or ICs (Section III-D), spintronic devices (Section III-E), and RTDs (Section III-F), are also described for the first time in Section III with exact engineering formulas, allowing for their optimization. For RTDs, the $1/f$ noise is found in Section III-F to be proportional to the squared voltage V_v for which the valley in the graph of the current occurs. It has a spectrum of 10^{-7} in amplitude for fractional current fluctuations at $V_v = 0.4$ V.

Section IV is dedicated to quantum $1/f$ phase noise in ultrasmall bulk acoustic wave (BAW) and surface acoustic wave (SAW) quartz resonators (Section IV-A–IV-C), or silicon MEMS resonators (Section IV-D–IV-F) and the resulting detection thresholds when used in various applications, such as biological and chemical microsensors. The sensors and all BAW and SAW quartz resonators are optimized by making them either very small compared with the coherence length of phonons in the quartz, or very large. The classical sources of phase noise in quartz and MEMS or NEMS resonators are also discussed in Sections IV-E and IV-F, and used to find the optimal size in the very small (microresonator domain).

Finally, Section V returns to HFET/MODFET-based oscillators calculating the noise figure of an amplifier based on them, including both the channel and gate noise sources. On this basis, the quantum $1/f$ phase noise of the resulting oscillator is calculated analytically, and successfully applied to a practical oscillator constructed on this basis by the group of R. York and H. Xu at the University of California, Santa Barbara (UCSB), as part of the ultralow phase noise electronics MURI program. In general, the examples presented here indicate the way in which the quantum $1/f$ noise can be applied to arbitrary materials, devices, and systems of modern technology and science, both in the civil and military domain.

A. *Notion of Phase Noise in Oscillators and Their Components*

In modern civilian and military communications, in resonant sensors, in radar and electronic warfare (EW), phase noise limits system performance. A 10-dB reduction in the noise floor will reduce the bit-error rate by a factor of 10^{-6} in digital signal processing (DSP) systems that process real-time inputs in an aerospace environment. For example, a 24-dB reduction in the noise floor of the radar corresponds to a fourfold increase in range resolution. It is especially critical when the radar has to discern a small incoming missile against the background of clutter. The main contributors to phase noise in a solid-state system are active device nonlinearity, inherent $1/f$ noise in the semiconductor device, and other elements of the RF circuit. In order to successfully control the influence of these contributors, it is necessary to first understand the physics of phase noise, and then to proceed with the design of devices and systems to eliminate or minimize its deleterious effects. This paper is focused on the $1/f$ noise, its physical origins at all levels, and its direct manifestation as phase noise, mainly in nanotechnology. First, however, the classical notions of noise are introduced here. The quantum $1/f$ phase noise is discussed in Sections IV and V.

The tip of the rotating vector describing the ac or microwave voltage of an oscillator in the complex plane fluctuates due to various reasons. Thermal noise causes a diffusional random process in which the tip of the vector can fluctuate along the length of the vector, causing amplitude noise, and also perpendicular to the rotating vector, causing phase noise. The amplitude noise is limited in magnitude by the tendency of the oscillant system to relax to that amplitude of oscillation, where the losses are compensated by the driving source of energy. The phase noise of a free running oscillator, on the other hand, does not have this restoring mechanism; therefore, thermal noise left to itself will cause the phase to perform a random diffusion in which its variance grows proportional to time

$$\langle \Delta\phi^2 \rangle = 2Dt \tag{1.1}$$

where D is a phase diffusion constant. D is a measure of how fast the oscillator loses its phase information or how fast a statistical ensemble of like oscillators would evolve toward the random phase state. We can therefore suppress the amplitude noise by simply writing

$$V = V_o \cos\left[\omega_o t + \phi(t)\right]. \tag{1.2}$$

The autocorrelation function of V is

$$\langle V(t)V(t+\tau) \rangle = V_o e^{-Dt} \cos(\omega_o t) \tag{1.3}$$

and its Fourier transform yields the two-sided spectral power density

$$S_V(\omega) = \frac{V_o^2 D}{[(\Delta\omega)^2 + D^2]}. \tag{1.4}$$

The ratio of the spectral power density at the frequency $\omega_o \pm \Delta\omega$ to the total signal power $V_o^2/2$ is the phase noise spectral density L

$$L\{\Delta\omega\} \equiv \frac{S_V(\omega)}{\left[\frac{V_o^2}{2}\right]} = \frac{2D}{[(\Delta\omega)^2 + D^2]}. \tag{1.5}$$

It is usually given in decibels, and referred to as "phase noise" in dBc, i.e., cycles^2/hertz. This also represents the mean square phase fluctuation in units of 2π radians (in cycles) squared, per Hertz of modulation frequency f, $<(\Delta\phi/2\pi)^2>_f$. One obtains for this classical noise the Leeson formula

$$L(f_m) = 10\log\left[\frac{1}{2}\left(\left(\frac{f_0}{2Q_l f_m}\right)^2 + 1\right)\left(\frac{f_c}{f_m} + 1\right)\left(\frac{FkT}{P_s}\right)\right]. \tag{1.6}$$

Quantum $1/f$ noise is a quantum fluctuation and is of a different nature, because it modulates the cross sections and process rates defined in quantum mechanics. Therefore, it also imparts quantum fluctuations to the dissipative coefficients, such as resistance, conductance, recombination speed, the phase diffusion constant D, phonon transition rates, tunneling rates, etc. Therefore, it should be added to the above relation that contains the classical contributions

$$L(f_m) = 10\log\left[\frac{1}{2}\left(\left(\frac{f_0}{2Q_l f_m}\right)^2 + 1\right)\left(\frac{f_c}{f_m} + 1\right) \times \left(\frac{FkT}{P_s}\right) + \frac{f_0^2}{2f_m^2}\frac{1}{4Q_l^4}S_{\frac{\delta\gamma}{\gamma}}\right]. \tag{1.7}$$

Here Q_l is the loaded quality factor, f_0 is the resonance frequency, f_c is the flicker corner frequency of the device generating the oscillations, γ is the dissipation rate that causes the osillator's free oscillations to attenuate, and $S_\delta\gamma/\gamma$ is the spectral density of fractional fluctuations in the dissipation rate γ. P_s is the amplifier's input signal power, and F is its noise figure. The bracket [ ] in (1.7) is $S_\phi/2$. New quantum $1/f$ and classical phase noise is discussed along with the resulting optimization rules in Section IV.

In modern communication, radar, and EW systems, the complex frequency, bandwidth, and signal-to-noise ratio requirements make the direct conversion (or homodyne) transceiver architecture superior to the traditional heterodyne RF transceiver-based approach. However, because it converts signals directly to (or from) the baseband, the direct conversion transceiver demands ICs (and/or semiconductor devices) with *extremely low* $1/f$ *noise*. Additionally, because the gain provided by the low-noise amplifier (LNA) and the mixer is limited, the downconverted signal is very sensitive to $1/f$ noise of the LNAs, filters, and mixers. For example, the 95S-1 direct conversion radio produced by Rockwell Collins covers input channels from 30 KHz to 2 GHz and requires an extremely low noise skirt (-140 dBc/Hz) near the baseband. The direct transceiver performance is also strongly affected by the noise performance and/or the spurs-free-dynamic-range (SFDR) of the subsequent analog-to-digital (ADC) and digital-to-analog (DAC) converters, especially when the analog-digital interface is placed close to the sensor/antenna for utilizing advanced DSP technologies. To meet the signal level variances present in typical SIGINT collection scenarios, a dynamic range of approximately 80 dB is required. This is compatible with most SIGINT systems with a minimum detectable signal of -75 dBm and a maximum signal level of 0 dBm. Current state of the art in GaAs-based ADC technology is limited to 60 dB (12-b) at 1 GHz. This performance is constrained by the *aperture jitter* of the current GaAs HBT technology (about 0.1 ps). The aperture jitter is the sample-to-sample variation in aperture delays, which can only be reduced by further decreasing the semiconductors $1/f$ noise.

On the basis of the LH- formula, from a system designer's perspective, the strategy to minimize overall phase noise consists in general of five basic steps:

1) One has to: a) maximize the unloaded Q of the elements and the loaded Q of the circuit (Handel Q^{-4} law term) and b) maximize the reactive energy by using the highest possible RF voltage across the resonators. Since this is limited by the breakdown voltage, a wide-gap device like a GaN FET should be used, if possible.
2) One has to: a) select devices with a low corner frequency fc and use a circuit design that minimizes quantum $1/f$ noise and b) reduce phase perturbations by using high impedance devices such as GaN HFETs, where the signal-to-noise ratio can be made very high. Furthermore, high biasing the active device (with feedback techniques) can minimize the modulation of the I/O dynamic capacitance. The capacitance modulation causes amplitude-to-phase conversion and hence introduces phase noise.
3) Finally, one has to: a) select circuit topologies with lowest possible noise figures F and b) with the lowest possible quantum $1/f$ fluctuation of the dissipation γ present in the resonant system (oscillator).

Another important factor is understanding the large-signal properties of the devices and circuits, e.g., the noise upconversion and the degree to which the overall system noise is determined by the low-frequency noise of the device. The high impedance and high breakdown voltage in GaN based devices offer unique new opportunities for the design of ultralow phase noise amplifiers and systems. The design concepts will thus be drastically different from those used in the well-known GaAs counterparts.

II. NATURE OF $1/f$ NOISE; CONVENTIONAL AND COHERENT QUANTUM $1/f$ NOISE

$1/f$ noise, referred to as flicker noise in the early literature, was first observed by Johnson [6] and prevails in many semiconducting devices. This noise contains in general both fundamental and nonfundamental fluctuations. Nonfundamental quasi-$1/f$ like contributions include superposition of lorentzian generation–recombination noise spectra, with a distribution of τ_{n} [7], and mobility fluctuation. The fundamental $1/f$ noise is mainly quantum $1/f$ noise [8]–[13].

In collision-free devices (diodes and ballistic devices) the $1/f$ noise can be explained by accelerated electrons emitting Bremsstrahlung, which has a $1/f$-spectrum. This is caused by the feedback of the emitted photon on the decelerating electron, yielding

$$\left\langle (\Delta \mathsf{I})^2 \right\rangle = \frac{\alpha_H}{f} \frac{I^2}{N} \Delta \mathsf{f} \tag{2.1}$$

where N is the number of carriers in the system, and α_{H} is the Hooge parameter [14]

$$\alpha_{\mathsf{conv}} = \frac{4\alpha}{3\pi} \left(\frac{\Delta \mathbf{v}}{c} \right)^2 \tag{2.2}$$

Here α is the fine structure constant, $\Delta\mathbf{v}$ is the charge of carrier velocity along its path, and c is the light velocity [8]. A similar formula can also be applied to semiconductors in which the carrier transport is collision determined. This type of noise is of a basic nature, and is now referred to as conventional *quantum* $1/f$ *noise, caused by the conventional quantum* $1/f$ *effect*—[8], [15], [16].

There is another form of quantum $1/f$ noise that is dominant in samples or systems with a large number of carriers. It is coherent quantum $1/f$ noise, caused by the coherent quantum $1/f$ effect, given by (2.1) with

$$\alpha_{\mathsf{coh}} = 2\alpha/\pi. \tag{2.3}$$

The relation between the coherent and conventional components is clarified in Section II-D.

For other reviews, see Van der Ziel [17], [18] and Handel [11].

Fluctuations with a spectral density proportional to $1/f$ are found in a large number of systems in science, technology, and everyday life. These fluctuations are known as $1/f$ noise in general. They have first been noticed by Johnson [6] in early amplifiers, have limited the performance of vacuum tubes in the thirties and forties, and have later hampered the introduction of semiconductor devices.

$1/f$ noise is present as a limitation in most modern high-technology devices. It is present in the resonance frequency of quartz resonators, in SAW devices, in junction and MIS IR detectors, in SQUIDs, in electron beams, etc. Outside the domain of electrophysics, $1/f$ noise is present in the rate of radioactive decay, in the flow rate of sand in an hourglass. It was also found in the flux of cars on an expressway, in the frequency of sunspots, in the light output of quasars, in the flow rate of the Nile over the last 2000 years, in the water current velocity fluctuations at a depth of 3100 m in the Pacific ocean, and in the loudness and pitch fluctuations of classical music. It has also been found below 10^{-8} Hz in the angular velocity of the earth's rotation, and below 10^{-4} Hz in the relativistic neutron flux in the terrestrial atmosphere [19].

Today the nature of $1/f$ noise is well understood [9]–[11], [20]. There are nonfundamental spectra that are resembling $1/f$ noise over certain limited frequency intervals (e.g., in MOSFETs) and covering up the fundamental noise in some cases, and there is fundamental $1/f$ noise in general. The nonfundamental (accidental) $1/f$-like spectra are usually obtained as a fortuitous superposition of Lorentzian spectra of the form $1/(1+\omega^2\tau^2)$, arising from exponential decay processes with autocorrelation functions of the form $e^{-t/\tau}$. The fundamental $1/f$ spectra have been shown [20] by us in general to arise at low frequencies from the simultaneous presence of nonlinearity and dimensional homogeneity of a special kind. This simultaneous presence is expressed by our sufficient criterion [20] (*epistemological basis of* $1/f$ *spectra*). The criterion allows us to determine whether a system defined by an arbitrary set of nonlinear integro-differential equations will have a $1/f$ spectrum. This criterion can also be seen as a consequence of the idempotent property of $1/f$-like spectra with respect to autoconvolutions [20].

A special case of this fundamental $1/f$ noise is quantum $1/f$ noise, which is caused by the electrodynamical quantum $1/f$ effect (Q$1/f$E) [8]–[13], [20]–[25], [77], [78]. The Q$1/f$E is of great technical, scientific, and practical importance and has two limiting forms which are described with simple formulas, in more detail, below: *conventional* (for small devices) [8], [12], [13], [21]–[23], [77], [78] and *coherent* (for large devices) [24], [25] quantum $1/f$ effect.

The Q$1/f$E characterizes the form in which electrical charges, and matter (gravidynamical Q$1/f$E) in general, exist in space and time. It arises from the interaction of electrical charges with their field. The Q$1/f$E is therefore as fundamental as the notion of scattering, or as the notion of interaction (or "existence"). It was derived also from the quantum information theory [26].

Although it is a special case of fundamental $1/f$ noise, being caused by the simultaneous presence of nonlinearity and homogeneity in quantum electrodynamics at low frequencies, as defined by the sufficient criterion, it is the most fundamental from the ontological point of view. That is the point of view which constructs the universe from quarks and leptons, or, at a more fundamental level, based on string theory. In particular, the Q$1/f$E is more fundamental than thermal noise and modulates [8], [27] the level of Nyquist (or Johnson) noise in current or voltage (but not in available power) to yield the physical thermal noise.

Below, the Q$1/f$E is defined and derived in physical terms with references to more rigorous derivations. It is then applied to various scattering mechanisms in homogeneous semiconductors, to p-n junctions, and to frequency standards.

A. Conventional Quantum $1/f$ Effect

This effect [8]–[10], [12], [13], [20]–[23], [77], [78], is present in any cross section or process rate involving charged particles or current carriers. The physical origin of quantum $1/f$ noise is easy to understand. Consider, for example, Coulomb scattering of current carriers, e.g., electrons on a center of force. The scattered electrons reaching a detector at a given angle away from the direction of the incident beam are described by DeBroglie waves of a frequency corresponding to their energy. However, some of the electrons have lost energy in the scattering process, due to the emission of bremsstrahlung. Therefore, part of the outgoing DeBroglie waves is shifted to slightly lower frequencies. When we calculate the probability density in the scattered beam, we obtain also cross terms, linear both in the part scattered with and without bremsstrahlung. These cross terms oscillate with the same frequency as the frequency of the emitted bremsstrahlung photons. The emission of photons at all frequencies results, therefore, in probability density fluctuations at all frequencies. The corresponding current density fluctuations are obtained by multiplying the probability density fluctuations by the velocity of the scattered current carriers. Finally, these current fluctuations present in the scattered beam will be noticed at the detector as low-frequency current fluctuations and will be interpreted as fundamental cross-section fluctuations in the scattering cross section of the scatterer. While incoming carriers may have been Poisson distributed, the scattered beam will exhibit super-Poissonian statistics, or bunching, due to this new effect, which we may call the quantum $1/f$ effect. The quantum $1/f$ effect is thus a many-body or collective effect, at least a two-particle effect, best described through the two-particle wave function and two-particle correlation function.

Let us estimate the magnitude of the quantum $1/f$ effect semiclassically. We start with the classical (Larmor) formula $2q^2\mathbf{a}^2/3c^3$, for the power radiated by a particle of charge q and acceleration $\mathbf{a}$. The acceleration can be approximated by a delta function $\mathbf{a}(t) = \Delta\mathbf{v}\delta(t)$ whose Fourier transform $\Delta\mathbf{v}$ is constant and is the change in the velocity vector of the particle during the almost instantaneous scattering process. The one-sided spectral density of the emitted bremsstrahlung power $4q^2(\Delta\mathbf{v})^2/3c^3$ is therefore also constant. The number $4q^2(\Delta\mathbf{v})^2/3hfc^3$ of emitted photons per unit frequency interval is obtained by dividing with the energy hf of one photon. The probability amplitude of photon emission $[4q(\Delta\mathbf{v})^2/3hfc^3]^{1/2}e^{i\gamma}$ is given by the square root of this photon number spectrum, including also a phase factor $e^{i\gamma}$. Let ψ be a representative Schrödinger catalogue wave function of the scattered outgoing charged particles, which is a single-particle function, normalized to the actual scattered particle concentration. The beat term in the probability density $\rho = |\psi|^2$ is linear both in this bremsstrahlung amplitude and in the nonbremsstrahlung amplitude. Its spectral density will therefore be given by the product of the squared probability amplitude of photon emission (proportional to $1/f$) with the squared nonbremsstrahlung amplitude which is independent of f. The resulting spectral density of fractional probability density fluctuations is obtained by dividing with $|\psi|^4$ and is therefore

$$|\psi|^{-4}\mathsf{S}^2_{|\psi|}(f) = \frac{8q^2(\mathbf{\Delta v})^2}{3hfNc^3} = \frac{2aA}{fN} = j^{-2}\mathsf{S}_{\mathrm{j}}(f) \qquad (2.4)$$

where $\alpha = e^2/\hbar c = 1/137$ is the fine structure constant and $\alpha A = 4q^2(\Delta\mathbf{v})^2/3hc^3$ is known as the IR exponent in quantum field theory, and is known as the quantum $1/f$ noise coefficient, in electrophysics. The experimentally measured quantity depends on many superposition or averaging processes and is often called, for historical reasons, Hooge constant.

The spectral density of current density fluctuations is obtained by multiplying the probability density fluctuation spectrum with the squared velocity of the outgoing particles. When we calculate the spectral density of fractional fluctuations in the scattered current j, the outgoing velocity simplifies, and therefore (2.4) also gives the spectrum of current fluctuations $S_j(f)$, as indicated above. The quantum $1/f$ noise contribution of each carrier is independent, and therefore the quantum $1/f$ noise from N carriers is N times larger. However, the current j will also be N times larger, and therefore in (2.4) a factor N was included in the denominator, for the case in which the cross-section fluctuation is observed on N carriers simultaneously.

The fundamental fluctuations of cross sections and process rates are reflected in various kinetic coefficients in condensed matter, such as the mobility μ and the diffusion constant D, the surface and bulk recombination speeds s, and recombination times τ, the rate of tunneling j_t and the thermal diffusivity in semiconductors. Therefore, the spectral density of fractional fluctuations in all these coefficients is given also by (2.4).

When we apply (2.3) to a certain device, we first need to find out which are the cross sections σ or process rates that limit the current I through the device, or that determine any other device parameter P. Then we have to determine both the velocity change $\Delta\mathbf{v}$ of the scattered carriers and the number N of carriers simultaneously used to test each of these cross sections or rates. Further, (2.4) provides the spectral density of quantum $1/f$ cross section or rate fluctuations. These spectral densities are multiplied by the squared partial derivative $(\partial I/\partial\sigma)^2$ of the current, or of the device parameter P of interest, to obtain the spectral density of fractional device noise contributions from the cross sections and rates considered. After doing this with all cross sections and process rates, we add the results and bring (factor out) the fine structure constant α as a common factor in front. This yields excellent agreement with the experiment [17], [26], [28]–[30], in a large variety of samples [31]–[37], devices [38]–[43] and physical systems.

Equation (2.4) was also derived in second quantization [12], [22], using the commutation rules for boson field operators. For fermions, one repeats the calculation replacing in the derivation the commutators of field operators by anticommutators, which yields [12], [22]

$$\rho^{-2}S_\rho(f) = j^{-2}S_j(f) = \sigma^2 S_\sigma(f) = \frac{2\alpha A}{f(N-1)}. \qquad (2.5)$$

This causes no difficulties, since $N \geq 2$ for particle correlations to be defined, and is practically the same as (2.4), since usually $N \gg 1$. Equations (2.4) and (2.5) suggest a new notion of physical cross sections and process rates which contain $1/f$ noise, and express a fundamental law of physics, important in most high-technology applications [9], [10], [12].

We conclude that the conventional quantum $1/f$ effect can be explained in terms of interference beats. The interference is between the part of the outgoing DeBroglie waves scattered without bremsstrahlung energy losses above the detection limit (given in turn by the reciprocal duration T of the $1/f$ noise measurement) on one hand, and the various parts scattered with bremsstrahlung energy losses. There is more to it than that: exchange between identical particles is also important. This, of course, is just one way to describe the reaction of the emitted bremsstrahlung back on the scattered current. This reaction, itself an expression of the nonlinearity introduced by the coupling of the charged-particle field to the electromagnetic field, thus reveals itself as the cause of the quantum $1/f$ effect, and implies that the effect cannot be obtained with an independent boson model. The effect, just like the classical turbulence-generated $1/f$ noise [44], [45], is a result of the scale-invariant nonlinearity of the equations of motion describing the coupled system of matter and field. Ultimately, therefore, this nonlinearity is the source of the $1/f$ spectrum in both the classical and quantum form of the theory. We can say that the quantum $1/f$ effect is an IR divergence phenomenon, this divergence being the result of the same nonlinearity. The quantum $1/f$ effect is, in fact, the first time-dependent IR radiative correction. Finally, it is also deterministic in the sense of a well determined wave function, once the initial phases γ of all field oscillators are given. In quantum mechanical correspondence with its classical turbulence analog [44], [45], the new effect is therefore a quantum manifestation of classical chaos which we can take as the definition of a certain type of quantum chaos.

B. Elementary Application to Homogeneous Semiconductor Samples

In a homogeneous sample of length L, cross section A, volume $V = AL$, carrier mobility μ, carrier concentration n, and total number of carriers $N = nAL$, the conductance $C = n\mu eA/L$ and the resistance $R = 1/C$ will exhibit quantum $1/f$ fluctuations with a spectral density $S_{\delta C/C}$ of fractional fluctuations $\delta C/C = -\delta R/R$ given by

$$S_{\frac{\delta C}{C}}(f) = S_{\frac{\delta R}{R}}(f) = S_{\frac{\delta\mu}{\mu}}(f) = \frac{\alpha_o}{fN}. \qquad (2.6)$$

Size dependence: To calculate α_o we first evaluate the parameter $s = nA \cdot 5.5 \cdot 10^{-13}$ cm introduced in the theory section below. If $s \geq 1$, coherent quantum $1/f$ noise (see Section IV-C below) is observed with $\alpha_o = 2\alpha/\pi$.

If $s < 1$, (2.6) requires knowledge of $(\alpha_o)_{\text{conv}}$. The latter is calculated from (2.4) or (2.5) for each type of scattering which limits the mobility $\mu = e\tau/m^*$ of the carriers. Here τ is the mean collision time or scattering time of the carriers, and m^* is their effective mass. In terms of the mean frequency of collisions $\nu = 1/\tau = \sigma v n_i$, one obtains $\mu = e/\nu m^* = e/\sigma v n_i m^*$. Here v is the mean speed of the carriers between collisions, σ a scattering cross section, and n_i the concentration of scatterers.

Conventional $Q1/fE$ in the Mobility: In general, Matthiessen' rule allows us to write, in terms of mobility

$$\frac{1}{\mu} = \sum_j \frac{1}{\mu_j} \qquad (2.7)$$

where μ_j is the mobility which would be obtained if only the jth scattering mechanism would be present and would limit the mobility. Applying a quantum $1/f$ fluctuation to (2.7), squaring and averaging quantum mechanically and statistically, we obtain as a reasonable first approximation

$$\frac{\delta\mu}{\mu^2} = \sum_j \frac{\delta\mu_j}{\mu_{j^2}}; \quad S_{\frac{\delta\mu}{\mu}}(f) = \sum_j \left(\frac{\mu}{\mu_j}\right)^2 S_{\frac{\delta\mu}{\mu_j}}(f). \qquad (2.8)$$

Equation (2.5) yields the strongest conventional quantum $1/f$ noise for Umklapp scattering, followed by the f and g forms of intervalley scattering or intervalley with Umklapp (in indirect band gap semiconductors like Si and Ge only), followed by normal phonon scattering, by neutral impurity scattering and by ionized impurity scattering (that has lowest $1/f$ noise). The corresponding terms in (2.8) reflect this hierarchy only partially, because of the factors $(\mu/\mu_j)^2$ which gauge the importance of each of the scattering processes in limiting the resultant mobility. To gain physical insight, the conventional quantum $1/f$ effect present in the various scattering processes is just estimated below and is actually calculated in Section IV-D by taking into account the corrections introduced by the momentum distribution of the carriers and by the phonon distribution function at the temperature T.

Impurity Scattering: For instance, in the case of impurity scattering, one obtains $S_{\delta\mu/\mu}(f) = S_{\delta\sigma/\sigma}(f)$. The physical scattering cross section σ, in turn, exhibits the Q$1/f$E with the spectral density given by (2.4) and (2.5)

$$S_{\frac{\delta\sigma}{\sigma}}(f)_i = \left(\frac{4\alpha}{3\pi fN}\right)\left\langle\left[\frac{\mathbf{\Delta v}}{c}\right]^2\right\rangle \approx \left(3 \cdot \frac{10^{-3}}{fN}\right)\left(\frac{\hbar\Delta\mathbf{k}}{m^* c}\right)^2. \qquad (2.9)$$

The average quadratic velocity change of the electrons in a scattering process is smaller in impurity scattering than in lattice scattering which includes normal phonon scattering, intervalley scattering in indirect band gap semiconductors with several "valleys," and Umklapp scattering, as well as optical phonon scattering. The Coulomb/Rutherford or Conwell/Weiskopf scattering cross section is proportional to $1/|\Delta\mathbf{k}|^4$, which favors small-angle scattering. Nevertheless, there are a few larger angle scattering events which are most effective in limiting the mobility and which therefore are decisive in the exact evaluation of the Q$1/f$E coefficient as a slow function of n_i, the concentration of impurities, given in the theory section below. This corresponds approximately to assuming randomizing collisions

$$\left\langle(\mathbf{\Delta v})^2\right\rangle_i = 2\langle v^2\rangle = \frac{6\,k_B T}{m^*} \qquad (2.10)$$

although impurity scattering is not randomizing. With m_o representing the free electron mass, we obtain this way

$$S_{\frac{\delta\mu}{\mu}}(f)_i = S_{\frac{\delta\sigma}{\sigma}}(f)_i = \left(\frac{4\alpha}{3\pi f N}\right)\left\langle\left[\frac{6\,k_B T}{m^* c^2}\right]\right\rangle \approx \left(\frac{10^{-9}}{fN}\right)\left(\frac{T m_o}{4\,m^* 100\ \mathrm{K}}\right). \tag{2.11}$$

The quantum $1/f$ noise power present in impurity scattering is therefore proportional to T.

Normal Acoustic Phonon Scattering: For normal phonon scattering, the product $\sigma v n_i$ has to be replaced by the lattice scattering rate Γ, given by an effective number of phonons times the squared phonon scattering matrix element $|M|^2$. The latter exhibits quantum $1/f$ fluctuations, because the carriers emit bremsstrahlung photons in the scattering process. Therefore, if the mobility μ of electrons (of random velocity $v = \hbar k/m^*$) is limited by phonon scattering, we get

$$S_{\frac{\delta\mu}{\mu}}(f)_{ap} = S_{\frac{\delta\Gamma}{\Gamma}}(f)_{ap} = \left(\frac{4\alpha}{3\pi f N}\right)\left\langle\left(\frac{\hbar\Delta\mathbf{k}}{m^* c}\right)^2\right\rangle = \left(3\cdot\frac{10^{-3}}{fN}\right)\left\langle\left(\frac{\hbar\Delta\mathbf{q}}{m^* c}\right)^2\right\rangle. \tag{2.12}$$

Here $\Delta\mathbf{q}$ is the acoustic phonon momentum transfer in the scattering process and the brackets indicate the average value. Using the linear approximation of the acoustic phonon dispersion relation $E_q = v_s q\hbar$, with v_s denoting the speed of sound, we obtain for a thermal phonon with $E_q = k_B T/2$

$$\left\langle\left(\frac{\hbar\Delta\mathbf{q}}{m^* c}\right)^2\right\rangle = \left(\frac{k_B T}{2\,v_s m^* c}\right)^2 = 1.25\cdot 10^{-5}\left(\frac{m_o}{m^*}\right)^2 \tag{2.13}$$

We finally obtain

$$S_{\frac{\delta\mu}{\mu}}(f)_{ap} = \left(3.75\cdot\frac{10^{-8}}{fN}\right)\left(\frac{m_o}{m^*}\right)^2. \tag{2.14}$$

The mean square momentum change and the $1/f$ noise are much larger (e.g., 50 times) for acoustic phonon scattering, because impurity scattering is mainly small-angle scattering. A more rigorous treatment for the many types of scattering present in semiconductors, taking into account the corrections introduced by the momentum distribution of the carriers and the phonon distribution function at the temperature T, is given in the theory section below in the second half of this paper for the case of silicon.

Umklapp Scattering: In this case, the momentum change is close to the smallest reciprocal lattice vector approximated by $\hbar G = 2\pi\hbar/a$, where a is the lattice constant. Therefore, (2.10) yields

$$(\alpha_{oU})_{\mathrm{conv}} = \left(\frac{4\alpha}{3\pi}\right)\left[\frac{2\pi\hbar}{am^* c}\right]^2 = \left(\frac{6\cdot 10^{-8}}{fN}\right)\left(\frac{m_o}{m^*}\right)^2 \tag{2.15}$$

for Umklapp scattering.

Intervalley Scattering: In indirect band gap semiconductors, the location of the energy minima of the conduction band in k-space is different from the location of the valence band energy maxima. In thermal equilibrium, electrons and holes are present close to the minima of the conduction and valence bands. Scattering processes carrying electrons from one minimum (or valley) to the other are known as intervalley scattering. This is large-angle scattering, compared with normal (intravalley) scattering, and it is therefore affected by larger conventional quantum $1/f$ noise, almost as large as Umklapp scattering. Indeed, e.g., in Si the eight minima are located at 0.85 G from the origin, where G is the smallest reciprocal lattice vector. For g-processes which scatter an electron to the valley symmetrically located on the other side of the origin, (2.15) remains valid with a correction factor of $(0.85)^2$. On the other hand, for f-processes in Si, scattering electrons between to neighboring valleys, the factor is two times smaller. There is also the possibility of intervalley scattering with Umklapp, which requires a correction factor of $(1-0.85)^2$. Equation (2.15) thus yields for intervalley scattering with Umklapp

$$(\alpha_{oIU})_{\mathrm{conv}} = 0.0225\left(\frac{4\alpha}{3\pi}\right)\left[\frac{2\pi\hbar}{am^* c}\right]^2 = \left(1.35\cdot\frac{10^{-9}}{fN}\right)\left(\frac{m_o}{m^*}\right)^2. \tag{2.16}$$

While this appears to indicate a lower contribution from these intervalley Umklapp processes, the corresponding $(\mu/\mu_j))^2$ factor in (2.8) insures a larger contribution to the resulting spectral density of quantum $1/f$ noise $S_{\delta\mu/\mu}(f)$. Physically, this is caused by the scarcity of high-energy phonons able to bridge the momentum gap of 0.85 G.

C. *Physical Derivation of the Coherent Quantum $1/f$ Effect*

This effect arises in a beam of electrons (or other charged particles propagating freely in vacuum) from the definition of the physical electron as a bare particle plus a coherent state of the electromagnetic field [24]. It is caused by the energy spread characterizing any coherent state of the electromagnetic field oscillators, an energy spread which spells nonstationarity, i.e., fluctuations. To find the spectral density of these inescapable fluctuations which are known to characterize any quantum state which is not an energy eigenstate, we use an elementary physical derivation based on Schrödinger's definition of coherent states. This supplements a rigorous derivation [9], [10], [20] which was given from a well-known quantum-electrodynamical propagator.

The coherent quantum $1/f$ effect will be derived [24] in three steps. First, we consider a hypothetical world with just one single mode of the electromagnetic field coupled to a beam of charged particles; considering the mode to be in a coherent state, we calculate the autocorrelation function of the quantum fluctuations in the particle-density (or concentration) which arise from the nonstationarity of the coherent state. Then we calculate the amplitude with which this one mode is represented in the field of an electron, according to electrodynamics. Finally, we take the product of the autocorrelation functions calculated for all modes with the amplitudes found in the previous step.

Let a mode of the electromagnetic field be characterized by the wave vector $\mathbf{q}$, the angular frequency $\omega = cq$, and the polarization λ. Denoting the variables $\mathbf{q}$ and λ simply by q in the labels of the states, we write the coherent state of amplitude $|z_q|$ and phase arg z_q in the form

$$\begin{aligned} |z_q\rangle &= \exp\left[-\left(\frac{1}{2}\right)|z_q|^2\right]\exp\left[z_q a_q^+\right]|0\rangle \\ &= \exp\left[-\left(\frac{1}{2}\right)|z_q|^2\right]\frac{\sum_{n=0}^{\infty}|z_q|^n}{n!|n\rangle}. \end{aligned} \tag{2.17}$$

Here a_q^+ is the creation operator which adds one energy quantum to the energy of the mode q. Let us use a representation of the energy eigenstates in terms of Hermite polynomials $H_n(x)$

$$|n\rangle = (2^n n!\sqrt{\pi})^{-\frac{1}{2}}\exp\left[-\frac{x^2}{2}\right]H_n(x)e^{in\omega t}. \tag{2.18}$$

This yields for the coherent state $|z_q\rangle$ the representation

$$\begin{aligned} \psi_q(x) &= \exp\left[-\left(\frac{1}{2}\right)|z_q|^2\right]\exp\left[-\frac{x^2}{2}\right]\sum_0^{\infty}\frac{[z_q e^{i\omega t}]^n H_n(x)}{[n!(2^n\sqrt{\pi})]^{\frac{1}{2}}} \\ &= \exp\left[-\frac{|z_q|^2}{2}\right]\exp\left[-\frac{x^2}{2}\right] \\ &\quad\times\exp\left[-z_q^2 e^{-2i\omega t} + 2xz_q e^{i\omega t}\right]. \end{aligned} \tag{2.19}$$

In the last form, the generating function of the Hermite polynomials was used. The summation extends to infinity at the upper limit. The corresponding autocorrelation function of the probability density function, obtained by averaging over the time t or the phase of z_q, is, for $|z_q| \ll 1$

$$\begin{aligned} P_q(\tau, x) &= \left\langle |\psi_q|_t^2 |\psi_q|_{t+\tau}^2 \right\rangle \\ &= \left\{1 + 8x^2|z_q|^2[1+\cos\omega\tau] - 2|z_q|^2\right\} \\ &\quad\times\exp\left[-\frac{x^2}{2}\right]. \end{aligned} \tag{2.20}$$

Integrating over x from $-\infty$ to ∞, we find the autocorrelation function

$$A^1(\tau) = (2)^{-\frac{1}{2}}\left\{1 + 2|z_q|^2\cos\omega\tau\right\}. \tag{2.21}$$

This result shows that the probability distribution contains a constant background with small superposed oscillations of frequency ω. Physically, the small oscillations in the total probability describe self-organization or bunching of the particles in the beam. They are thus more likely to be found in a measurement at a certain time and place than at other times and places relative to each other along the beam. Note that for $z_q = 0$ the coherent state becomes the ground state of the oscillator which is also an energy eigenstate, and therefore stationary and free of oscillations.

We now determine the amplitude z_q with which the field mode q is represented in the physical electron. One way to do this is to let a bare particle dress itself through its interaction with the electromagnetic field, i.e., by performing first-order perturbation theory with the interaction Hamiltonian

$$H' = A_\mu j^\mu = -\left(\frac{e}{c}\right)\mathbf{v}\bullet\mathbf{A} + e\phi \tag{2.22}$$

where $\mathbf{A}$ is the vector potential and ϕ the scalar electric potential. Another way is to Fourier expand the electric potential e/r of a charged particle in a box of volume V. In both ways we obtain the well-known result

$$|z_q|^2 = \pi\left(\frac{e}{q}\right)^2(\hbar cqV)^{-1}. \tag{2.23}$$

Considering now all modes of the electromagnetic field, we obtain from the single-mode result of (2.21)

$$\begin{aligned} A(\tau) &= C\Pi_q\left\{1 + 2|z_q|^2\cos\omega_q\tau\right\} \\ &= C\left\{1 + \Sigma_q 2|z_q|^2\cos\omega_q\tau\right\} \\ &= C\left\{1 + 4\left(\frac{V}{2^3\pi^3}\right)\int d^3q|z_q|^2\cos\omega_q\tau\right\} \end{aligned} \tag{2.24}$$

Here we have again used the smallness of z_q, and we have introduced a constant C. Using (2.23) we obtain

$$\begin{aligned} A(\tau) &= C\left\{1 + 4\pi\left(\frac{V}{2^3\pi^3}\right)\left(\frac{4\pi}{V}\right)\left(\frac{e^2}{\hbar c}\right)\int\left(\frac{dq}{q}\right)\cos\omega_q\tau\right\} \\ &= C\left\{1 + \frac{2\left(\frac{\alpha}{\pi}\right)\int\cos(\omega\tau)d\omega}{\omega}\right\}. \end{aligned} \tag{2.25}$$

Here $\alpha = e^2/\hbar c$ is Sommerfeld's fine structure constant 1/137. The first term in curly brackets is unity and represents the constant background, or the dc part of the current carried by the beam of particles through vacuum. The autocorrelation function for the relative (fractional) density fluctuations, or for the current density fluctuations in the beam of charged particles is obtained therefore by dividing the second term in curly brackets by the first term. The constant C drops out when the fractional fluctuations are considered. According to the Wiener–Khintchine theorem, the coefficient of $\cos\omega\tau$ is the spectral density of the fluctuations $S_{|\psi|}^2$ for the particle concentration, or S_j for the current density $j = e(k/m)|\psi|^2$

$$S_{|\psi|}^2\left\langle|\psi|^{-2}\right\rangle = S_j\langle j\rangle^{-2} = 2\left(\frac{\alpha}{\pi f N}\right) = 4.6\cdot 10^{-3}f^{-1}N^{-1}. \tag{2.26}$$

Here we have included the total number N of charged particles which are observed simultaneously in the denominator, because the noise contributions from each particle are independent. This is the coherent Q1/fE. It is related to the conventional Q1/fE introduced above in Sections II-A and B. Equation (2.26) was also derived directly [9]–[11], [20], from the well-known physical QED propagator of Kulish, Faddeev, and Zwanziger.

D. Relation Between Coherent and Conventional Quantum $1/f$ Effect

We turn now to the connection [25] with the conventional Q1/fE. The coherent state in a conductor or semiconductor sample is the result of the experimental efforts directed toward establishing a steady and constant current and is therefore the state defined by the collective motion, i.e., by the drift of the current carriers. It is expressed in the Hamiltonian by the magnetic energy $E = m$, per unit length, of the current carried by the sample. In very small samples or electronic devices, this magnetic energy

$$E_m = \int \left(\frac{B^2}{8\pi}\right) d^3x = \left[\frac{nevS}{c}\right]^2 \left[\frac{1}{4} + \ln\left(\frac{R}{r}\right)\right] \tag{2.27}$$

is much smaller than the total kinetic energy E_k of the drift motion of the individual carriers

$$E_k = \frac{\sum mv^2}{2} = \frac{nSmv^2}{2} = E_m/s. \tag{2.28}$$

Here we have introduced the magnetic field B, the carrier concentration n, the cross-sectional area S and radius r of the cylindrical sample (e.g., a current carrying wire), the radius R of the electric circuit, and the "coherence ratio"

$$\begin{aligned} s &= \frac{E_m}{E_k} = \frac{2ne^2S}{mc^2\left[\frac{1}{4} + \ln\left(\frac{R}{r}\right)\right]} \approx 2e^2\, N'/mc^2 \\ &= 2N'r_o = 5.68 \cdot 10^{-13}\ \mathrm{cm} \cdot N' \end{aligned} \tag{2.29}$$

where $N' = nS$ is the number of carriers per unit length of the sample, $r_o = e^2/mc^2 = 2.84 \cdot 10^{-13}$ cm is the classical radius of the electron, and the expression in rectangular brackets has been approximated by unity in the last form. We expect the total observed spectral density of the mobility fluctuations to be approximated by a relation of the form

$$\left(\frac{1}{\mu^2}\right) S_\mu(f) = \left[\frac{1}{(1+s)}\right]\left[\frac{2\alpha A}{fN}\right] + \left[\frac{s}{(1+s)}\right]\left[\frac{2\alpha}{\pi f N}\right] \tag{2.30}$$

which can be interpreted as an expression of the effective Hooge constant if the number N of carriers in the (homogeneous) sample is brought to the numerator of the left-hand side. In this equation, $\alpha A = 2\alpha(\Delta v/c)^2/3\pi$ is the usual nonrelativistic expression of the IR exponent, present in the familiar form of the conventional quantum $1/f$ effect [8]–[13], [20]–[22]. This equation is limited to quantum $1/f$ mobility (or diffusion) fluctuations and does not include the quantum $1/f$ noise in the surface and bulk recombination cross sections [46], in the surface and bulk trapping centers [47]–[49],

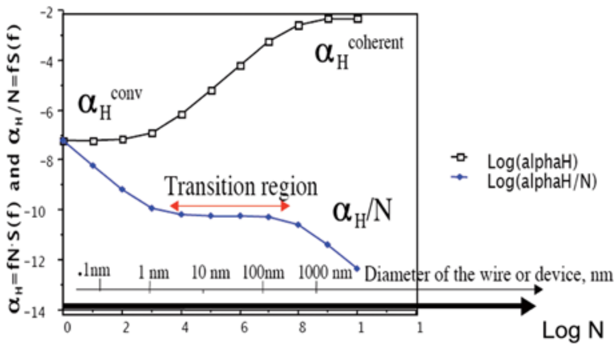

Fig. 1. Q1/f parameter α_H and spectrum of fractional mobility fluctuations $fS_{\delta\mu/\mu} \equiv \alpha_H/N$ shown as a function of the number N of carriers in the sample. The transition region, in which we observe the proximity effect, is marked by a red arrow. The wire diameter scale gets shifted to the right (or left) proportionally when the concentration of carriers increases (or decreases) from the assumed value of 10^{17} cm^{-3}. We took the cross section to be (140 nm^2), the length 5 mm, and the concentration $n = 10^{17}$ cm^{-3} as an example. The flat portion of the lower curve explains why $1/f$ noise was less of a problem during the past miniaturization stage. It is now again a problem, as the increase below $\log N = 3$ shows.

in tunneling and injection processes [17], [18], [28], [29], in emission, or in transitions between two solids [50]–[54].

Note that the coherence ratio s introduced here equals the unity for the critical value $N' = N'' = 2 \cdot 10^{12}$/cm, e.g., for a cross section $S = 2 \cdot 10^{-4}$ cm^2 of the sample when $n = 10^{16}$. For small samples with $N' \ll N''$, only the first term survives, while for $N' > N''$ the second term in (2.30) is dominant shown as a function of the number N of carriers in the sample. The transition region (shown in Fig. 1), in which we observe the proximity effect, is marked by a red arrow. The wire diameter scale gets shifted to the right (or left) proportionally when the concentration of carriers increases (or decreases) from the assumed value of 10^{17} cm^{-3}. We took the cross section to be (140 nm^2), the length 5 mm, and the concentration $n = 10^{17}$ cm^{-3} as an example. The flat portion of the lower curve explains why $1/f$ noise was less of a problem during the past miniaturization stage. It is now again a problem, as the increase below $\log N = 3$ shows.

Case of HFETs and FETs of Large Width: Finally, an important special case should be mentioned. Equation (2.27) was derived for the case of a cylindrical sample with circular cross section of radius r, shaped like a straight wire. Modern FETs and HFETs try to increase the denominator N in (2.30) without markedly increasing the coherence parameter s by choosing an extreme case of a rectangular cross section for the portion between source and drain, and even more extreme for the channel, which is the region under the gate. Indeed, the circular cross section is replaced by a rectangle with a very large width w of several hundreds of micrometers and less than a micrometer thick, the channel being even thinner. The channel is reduced to a two-dimensional (2-D) quantum sheet, which is a quantum well of size (thickness) t in the 3rd dimension, toward the gate. Most important, the "length" L_{DS} of the source-to-drain distance is only of the order of 1 μm, while the gate length is just about a quarter of a micrometer or less. In this case, the kinetic energy E_k per unit length in the direction of L_{DS} is still given by (2.28),

Table 1
Comparison of Theoretical $Q1/f$ α Values With Experiment Shown in Fig. 2

	Markers						
$V_G{}^*/1V$		1	2	3	3.45	4.25	5
$I_{DS}/1mA$			1.9	2.55	3.1	3.8	4.9
$\alpha_H{}^{theor} \cdot 10^5$	+	2.95	3.6	5.0	7.0	9.91	16 (Eq. 3.15)
$\alpha_H{}^{exp} \cdot 10^5$	x		4.9	4.2	11	16.0	17

$$\alpha_H{}^{theor} \equiv [fS_V/V^2]\, L^2/Re\mu = \frac{I_{ch}L^2}{qV_{DS}^2\mu^2}\left\{\frac{\alpha_H^{coh} I_{ch}}{qZ^2D_{eff}^2 V_{th}V_{DS}} + \frac{\alpha_H^{conv} q v_s^2}{I_{ch}}\left(1 - \frac{V_G^*}{V_{DS}} + \frac{V_{th}}{V_{DS}}\right)\right\} \equiv$$

$$\frac{L^2}{1\mu^2}\bullet\left(\frac{92.4\, cm^2/V\cdot s}{\mu_{eff}}\right)^2\bullet\left(\frac{5V}{V_{DS}}\right)^2\left\{2.4\cdot10^{-5}\left(\frac{50\mu}{Z}\right)^2\frac{5V}{V_{DS}}\left(\frac{I}{1.9mA}\right)^2 + 1.95\cdot10^{-5}\,\frac{\alpha_H^{conv}}{4.1\cdot10^{-6}}\left(\frac{v}{10^7 cm/s}\right)^2\left(1-\frac{V_G^*}{V_{DS}}+\frac{V_{th}}{V_{DS}}\right)\right\}$$

but the magnetic energy E_m per unit length in the direction of $L_{\rm DS}$ is roughly proportional with the first power of w only, instead of w^2, and can be approximated by

$$E_m = \frac{\pi\left[\ln\left(\frac{w}{2L_{\rm DS}}\right)\right] L_{\rm DS}\left[\frac{\rm nevS}{c}\right]^2}{w}. \tag{2.31}$$

This indicates decoherence along the device width w. For $w \gg L_{\rm DS} > t$, this yields a coherence ratio

$$s \approx \pi n r_o t L_{\rm DS} \ln\left(\frac{w}{2L_{\rm DS}}\right) \quad \text{for} \quad w \gg L_{\rm DS} > t \tag{2.32}$$

which shows that only an effective width $w = w_{\rm eff}$ about equal to $L_{\rm DS}$ should be used in the calculation of the coherence parameter s in this special case; larger widths are subject to decoherence, i.e., their magnetic energy no longer increases proportional to w^2, or N'^2. This favors lower, mainly conventional, quantum $1/f$ noise in these devices, in spite of the large values of w, in agreement with the practical results, which anticipated the quantum $1/f$ result simply by trial and error, unaware of the subtleties of the transition from coherent to conventional $Q1/f$ noise in this case, and in general. It also shows that fragmentation of the extremely large widths w does not reduce $1/f$ noise in this special case.

Note: To derive the rough approximation given in (2.31), one writes the expression of the coherent ($\propto n^2$) contribution of the currents in the short but very wide channel to the magnetic energy of the circuit in the form

$$\begin{aligned} E_m &= \int\left[\mathbf{j}(\mathbf{x})\cdot\frac{\mathbf{j}(\mathbf{x}')}{2c^2|\mathbf{x}-\mathbf{x}'|}\right]d^3x d^3x' \\ &= e^2v_d^2\int\left[n(\mathbf{x})\cdot\frac{n(\mathbf{x}')}{2c^2|\mathbf{x}-\mathbf{x}'|}\right]d^3xd^3x'. \end{aligned} \tag{2.33}$$

The integral coincides with the electrostatic energy of an equivalent constant charge density numerically equal to e/c^2

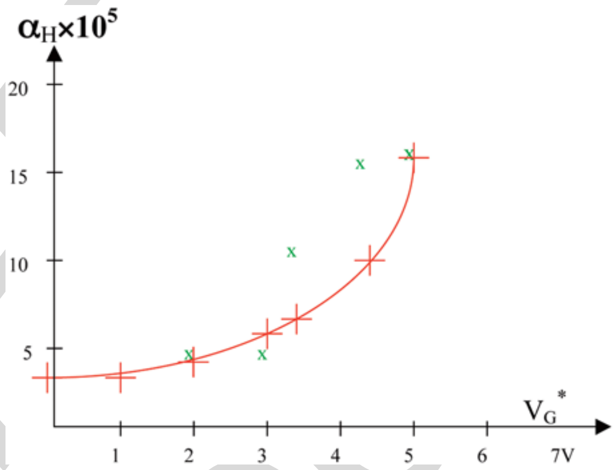

Fig. 2. Comparison of the quantum $1/f$ first principles results + with the experimental results **x** of Balandin *et al.*, in "Flicker noise in GaN/AlGaN doped channel heterostructure FETs," *IEEE Electron Device Lett.*, , vol. 19, no. 12, pp. 475–477, Dec. 1998. Ignoring (2.32) yields the errors seen at larger V_{GS}.

in CGS, or $e\mu_o/4\pi\varepsilon_0$ in SI, uniformly distributed over the volume $wtL_{\rm DS}$ of the channel. This energy, in turn, is calculated as the corresponding volume integral over the squared equivalent electric field, using $L_{\rm DS}$ as a lower cutoff. The equivalent electric field is netw/cr$(r^2 + w^2/4)^{1/2}$ at a distance r in the median plane of a segment of length w oriented along the width w of the channel. A more elaborate calculation does not simply approximate the field with its value in this median plane, but yields similar results in the end. Equations (2.31) and (2.32) explain the discrepancy at larger V_{GS}^* in Table 1 and Fig. 2.

III. Quantum $1/f$ Noise in GaN/AlGaN HFETs and RTDs

A. Introduction to HFETs

AlGaN/GaN HFETs have remarkable initial performance, but degrade appreciably over time, mainly due to a drop in 2-D electron gas mobility. Moreover, the output characteristic compression at high frequencies hinders power and power-added efficiencies. This is a case in point demonstrating the pitfalls of neglecting materials defects on the way to production of devices. Another related observation is that the Hall mobility in the best bulk GaN is well below 1000 $\mathrm{cm}^2/\mathrm{Vs}$, whereas in modulation doped structures, it approaches 2000 $\mathrm{cm}^2/\mathrm{Vs}$ at room temperature. What is also vitally important is the high resistivity or semi-insulating material, which is used for buffer layers where the 2DEG layer is actually formed. The quality of this layer along with the AlGaN layer determines the performance, stability, and reliability of a modulation doped HFET. A question is, what is the best route toward semi-insulating materials?

At this stage of development, the major device problems are truly materials and design problems, and these are precisely the issues that we are studying with the quantum $1/f$ approach.

This paper applies the quantum theory of $1/f$ noise to predict the $1/f$ amplitude and phase fluctuations measured on GaN-doped channel HFETs, to compare the measured values of the effective Hooge parameter with the theoretical value, and to do the device optimization.

To apply the theory, the HFET channel is first considered here to be similar to a parallelepipedic sample of typical dimensions of 50-μm gate width, 500-Å channel depth, and 1-μm gate length. In second approximation, the reduction in channel conductivity from source to drain is also taken into account, in order to find the effective quantum $1/f$ parameter that is to be compared with the measured Hooge parameter. In the uniform channel approximation, we expect from the 2 10^{17} cm^{-3} doping level a number of electrons per unit channel length of

$$N' = 50\ \mu\mathrm{m} \times 0.05\ \mu\mathrm{m} \times 2\ 10^{17}\ \mathrm{cm}^{-3} = 5\ 10^{9}\ \mathrm{cm}^{-1} \tag{3.1}$$

at flatband. This allows us to find the "s"-parameter present in the general quantum $1/f$ formula. *This "coherence parameter" is the number of charge carriers in a thin salami-slice-like section of the sample*. "Thin" means twice the classical radius $r_o = e^2/mc^2 = 2.84\ 10^{-13}$ cm of the electron. In our case, the parameter is

$$s = 2 \times 5\ 10^{9}\ \mathrm{cm}^{-1} \times 2.84\ 10^{-13}\ \mathrm{cm} = 2.84\ 10^{-3}. \tag{3.2}$$

Knowledge of the coherence parameter $s = N'r_o$ allows for the calculation of the quantum $1/f$ noise parameter in the general nonuniform channel case, with $N = N'(y)$

$$\begin{aligned}\alpha_H &= \frac{[s\alpha_{\mathrm{coh}} + \alpha_{\mathrm{conv}}]}{(1+s)} \\ &= \left[\frac{2}{137\pi(1+s)}\right]\left\{s + \left(\frac{2}{3}\right)\left(\frac{\Delta \mathbf{v}}{c}\right)^2\right\}.\end{aligned} \tag{3.3}$$

The terms in curly brackets correspond to the coherent and conventional quantum $1/f$ effect contributions, respectively. The effective velocity change Δv of the current carriers is present in the conventional term, and the fine structure constant $\alpha = e^2/\hbar c = 1/137$ in both terms, as required by the well known quantum $1/f$ formulas [55].

B. *Theory of Quantum $1/f$ Noise in AlGaN/GaN HFETs*

The element of resistance dR along the current can be written

$$dR = \frac{dy}{(q\mu_n N')} \tag{3.4}$$

where μ_n is the electron mobility. The quantum $1/f$ noise in the element of resistance dR is given by the basic quantum $1/f$ formula for mobility fluctuations [55]

$$\frac{\left\langle (\delta dR)^2 \right\rangle_f}{(dR)^2} = \frac{\alpha_H}{f dN} \tag{3.5}$$

where $dN = N'dy$ is the number of carriers in the element of length dy along the channel. Using (3.4) for dR, we obtain

$$f\left\langle (\delta dR)^2 \right\rangle_f = \left[\frac{dR dy}{q\mu_n N'}\right]\frac{\alpha_H}{dN}. \tag{3.6}$$

Multiplying on both sides with the channel current

$$I_{\mathrm{ch}} = -\frac{dV}{dR} \tag{3.7}$$

and integrating yields

$$f I_{\mathrm{ch}}\left\langle (\delta R)^2 \right\rangle_f = -\int_{Vs}^{Vd}\left[\frac{dV}{q\mu_n N'^2}\right]. \tag{3.8}$$

Introducing Fermi statistics, for a GaN/$\mathrm{Al}_x\mathrm{Ga}_{1-x}\mathrm{N}$ doped n-channel HFET, the number of carriers per unit length N' of the 2-D channel is written in the form

$$N'(y) = Z D_{\mathrm{eff}} V_{\mathrm{th}} \log\left\{1 + \exp\left[\frac{(V_G^* - V(y))}{V_{\mathrm{th}}}\right]\right\}. \tag{3.9}$$

Here $D_{\mathrm{eff}} = qm/\pi\hbar$ is q times the effective density of states per unit area. Multiplying (3.13) by I/f, this yields the spectral density of V_{DS} fluctuations in terms of device width Z, channel current I, and thermal voltage $V_{\mathrm{Th}} = kT/q$

$$\begin{aligned}\left\langle (\delta V_{\mathrm{DS}})^2 \right\rangle_f &= \frac{|I|}{f Z^2 D_{\mathrm{eff}} q V_{\mathrm{th}}} \\ &\quad \times \int_{X_0}^{X_1}\left(\frac{\alpha_H}{\mu_n}\right)\left[\frac{dX}{(X-1)\ln^2 X}\right]\end{aligned} \tag{3.10}$$

$$X \equiv 1 + \exp\left(\frac{V_G^* - V}{V_{\mathrm{th}}}\right). \tag{3.11}$$

Here X_0 and X_1 are the values of X at the source ($V = 0$) and at the drain ($V = V_{\mathrm{DS}}$), while $\alpha_H = \alpha_H(y)$ is a y-dependent form of the quantum $1/f$ coefficient introduced in (3.3) above. For $(V_G^* - V)/V_{\mathrm{th}} \ll 1$

$$X - 1 = \frac{(V_G^* - V)}{V_{\mathrm{th}}} \tag{3.12}$$

and the linear approximation of (3.11)–(3.13) is regained for a 2-D quantized channel.

In general, part of the channel may be subthreshold, starting at $V(y) = V_{\mathrm{sat}} = V_G*$. In that case, the use of Fermi statistics becomes unavoidable, as is shown in (3.10). However, although (3.10) includes the field dependence of α and μ, it fails to reflect the physical situation correctly, because it neglects the impact ionization effect in the subthreshold section of the channel length.

Using the fact that the velocity of the carriers shows strong saturation in the subthreshold section, to include the impact ionization effect, we return to the variable V in (3.10), split up the integral at $V(y) = V_G * - V_{\mathrm{th}}$, and write the second, subthreshold, part of the integral separately, with the number of carriers per unit channel length defined as $N' = I_{\mathrm{ch}}/qv_s$, where v_s is the saturation velocity

$$\begin{aligned} &fI_{\mathrm{Ch}} \left\langle (\delta R)^2 \right\rangle_f \\ &= \int_0^{V_{\mathrm{sat}}} \frac{\alpha_{\mathrm{coh}} dV}{q\mu N'^2} + \int_{V_{\mathrm{sat}}}^{V_{\mathrm{DS}}} \frac{\alpha_{\mathrm{conv}} q v_s^2 dV}{q\mu I_{\mathrm{Ch}}^2} \\ &\approx \frac{\sqrt{2}}{q\mu} \int_0^{V_{\mathrm{DS}}} \frac{\alpha_H(N') dV}{\frac{I_{\mathrm{Ch}}^2}{q^2 v_s^2} + Z^2 D_{\mathrm{eff}}^2 V_{\mathrm{th}} \ln\left\{1 + \exp\left[\left(\frac{V_G^* - V}{V_{\mathrm{th}}}\right)\right]\right\}}. \end{aligned} \tag{3.13}$$

Here α was approximated by its coherent value, α_{coh} in the above-threshold term. We also can approximate the ratio $v(E)/E$ by 3.5 μ_0, where μ_o is the low-field mobility, and E is the electric field strength. The last form in (3.13) is an approximation in which the two denominators are added, allowing the larger one to prevail automatically, but keeping α in the general form given by (3.3). By multiplying both terms of the middle form of (3.13) with $I_{\mathrm{ch}}/(V_{\mathrm{DS}})^2$, one obtains for the spectral density of fractional fluctuations in V_{DS}

$$\begin{aligned} &fV_{\mathrm{DS}}^{-2} \left\langle (\delta V_{\mathrm{DS}})^2 \right\rangle_f \\ &= \left(\frac{I_{\mathrm{Ch}}}{V_{\mathrm{DS}}^2}\right) \int_0^{V_{sat}} \frac{\alpha_{\mathrm{coh}} dV}{q\mu N'^2} + \int_{V_{\mathrm{sat}}}^{V_{\mathrm{DS}}} \frac{\alpha_{\mathrm{conv}} q v_s^2 dV}{V_{\mathrm{DS}}^2 q\mu I_{\mathrm{Ch}}} \\ &= \frac{1}{V_{\mathrm{DS}}\mu} \left\{ \frac{\alpha_H^{\mathrm{coh}} I_{\mathrm{ch}}}{qZ^2 D_{\mathrm{eff}}^2 V_{\mathrm{th}} V_{\mathrm{DS}}} + \frac{\alpha_H^{\mathrm{conv}} q v_s^2}{I_{\mathrm{ch}}} \right. \\ &\qquad \left. \times \left(1 - \frac{V_G^*}{V_{\mathrm{DS}}} + \frac{V_{\mathrm{th}}}{V_{\mathrm{DS}}}\right) \right\}. \end{aligned} \tag{3.14}$$

The second term in curly brackets must be omitted when negative. Multiplying this expression with $L^2/Rq\mu$, one finds a theoretical expression

$$\begin{aligned} \alpha_{\mathrm{theor}} = \frac{I_{\mathrm{ch}} L^2}{qV_{\mathrm{DS}}^2 \mu^2} &\left\{ \frac{\alpha_H^{\mathrm{coh}} I_{\mathrm{ch}}}{qZ^2 D_{\mathrm{eff}}^2 V_{\mathrm{th}} V_{\mathrm{DS}}} \right. \\ &\left. + \frac{\alpha_H^{\mathrm{conv}} q v_s^2}{I_{\mathrm{ch}}} \left(1 - \frac{V_G^*}{V_{\mathrm{DS}}} + \frac{V_{\mathrm{th}}}{V_{\mathrm{DS}}}\right) \Theta() \right\} \end{aligned} \tag{3.15}$$

for the experimental Hooge constant defined in the usual way by the simple uniform-channel expression $\alpha_{\mathrm{exp}} \equiv [fS_V/V^2]\, L^2/Re\mu\, R$ is here the channel resistance and $V_{G^*} = V_{GS} - V_T$. Here $\Theta()$ represents the step function of the quantity in the preceding brackets, defined to be zero for negative arguments and one for positive values.

C. Comparison With Measurements on AlGaN/GaN HHFETs

The experimental values α_{exp} measured at $V_{\mathrm{DS}} = 5$ V by Balandin *et al.* [32], [35], are 4.9, 4.2, 11, 16, and 17, in units of 10^{-5} corresponding to V_{G^*} values of 2, 3, 3.45, 4.25, and 5 V, respectively. Equation (3.15) yields in the same conditions the values α_{theor} shown in Table 1 and Fig. 2. The agreement is good, with no fudge factors or adjustable parameters.

We briefly present here the investigation of low-frequency noise through measurement of HFETs in St. Louis, MO. These devices were grown by Mishra *et al.* at UCSB on various substrates, SiC, sapphire, and HVPE. The experimental results are discussed and are compared with the quantum theory of $1/f$ noise.

Low-frequency noise can be described in terms of resistance fluctuations $\delta R/R$. If the current in a circuit is held constant, $\delta R/R$ equals the fractional voltage fluctuations $\delta V/V$ at the end of samples or device under study. We denoted the spectral density of fractional resistance fluctuations with $S_{\delta R/R}(f) = R^{-2} < (\delta R)^2 >_f$. The main experimental results are as follows.

1) At $Vg = 0$, the lowest $S_{\delta R/R}(f)$ was measured for an HFET on the SiC substrate with $S_{\delta R/R}(f) = 3.9 \cdot 10^{-13}$, followed by with $S_{\delta R/R}(f) = 2.0 \cdot 10^{-11}$ on sapphire, and the noisiest, with $S_{\delta R/R}(f) = 7.8 \cdot 10^{-11}$ on HVPE.
2) When Vg changes from 0 to -3.0 V for an HEFT on SiC, the $S_{\delta R/R}(f)$ increases from $1.24 \cdot 10^{-12}$ to $1.64 \cdot 10^{-10}$, about two orders of magnitude.

Agreement between the experimental values and the theory values is remarkable, as shown in Table 2 below. This research also indirectly proves that increasing the device channel width is very effective for decreasing the low-frequency noise. This is very important for high power density microwave generation.

The apparatus is shown in Fig. 3 below, a typical spectrum and background in Fig. 4.

D. Low-Frequency Noise in Bent Ultrathin Semiconductors

In ultrathin semiconductor devices, surface scattering can no longer be ignored and significantly lowers the mobility

Table 2

Substrate	R_{DS}/Ω	V_{DS}/V	$fS_{\delta R/R}$	α exp	αtheor
HVPE					
STD3	36	0.9	7.8E-11	0.99E-5	3.0E-5
Sapphire					
STD7	20.5	0.27	2.0E-11	2.06E-5	2.7E-5
SiC					
STD12	37.3	0.53	3.9E-13	2.69E-7	1.5E-7
STD4	40.4	2.1	1.24E-12	7.92E-7	3.3E-6

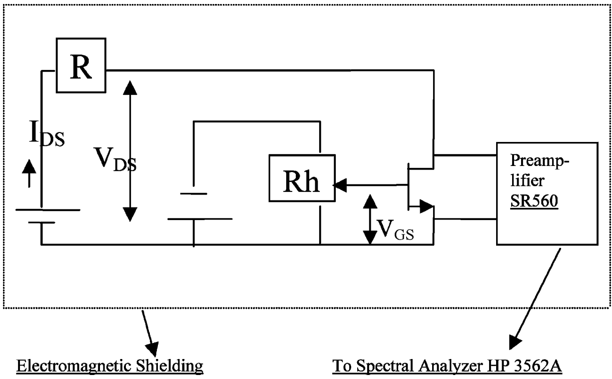

Fig. 3. Experimental setup. As shown in Fig. 1, the gate voltage V_G of the device under test is controlled with a Rheostat Rh. The devices were open, i.e., not capped.

of the carriers. This contributes a term in the scattering rate, which is proportional to λ/a in first approximation, where a is the thickness of the crystalline semiconductor sample. Since Umklapp and intervalley scattering are the main limitation on the mobility of current carriers in silicon, and since they are affected by the largest conventional quantum $1/f$ effect, we expect a $1/f$ noise reduction in properly fabricated ultrathin semiconductor samples.

Ultrathin silicon samples and devices are obtained at the University of California, Irvine, Microfabrication Laboratory in the Engineering Gateway building. One of the methods used by us involves uniform etching to reduce the thickness of the sample by an order of magnitude.

To estimate the conventional quantum $1/f$ effect (CQ$1/f$E) in ultrathin Si devices and ICs, we need to also include the effect of the reduction in carrier lifetime τ due to the surface recombination rate. This increases the $1/f$ noise in junction devices, because the quantum $1/f$ effect is inversely proportional to the number N of carriers which have participated in the generation–recombination-limited current transport through the various p-n junctions. This number is, however, given by the GR component of the current I multiplied by the lifetime τ of the carriers.

Assuming small samples, the CQ$1/f$E is applicable and is affecting surface scattering rates according to the fundamental formula

$$S_{\frac{\delta\Gamma}{\Gamma}} = \left(\frac{4\alpha}{3\pi}\right)\left\langle(\Delta\mathbf{v}/c)^2\right\rangle. \tag{3.16}$$

The brackets indicate a statistical average over the parameters of a surface scattering. We obtain the $1/f$ noise power spectrum by substituting a considerably increased thermal velocity for Δv, because of the surface potential ($V_o > 0$ in n-type) in the presence of an accumulation layer, which is not applicable for $V_o < 0$ (depletion in n-type material). However, the case of inversion would lead again to a $1/f$ noise increase in spite of $V_o < 0$, but there is also a carrier identity switch which affects the result in this case, due to the difference in effective mass and scattering mechanism.

Surface Scattering and Bulk Scattering: The total scattering rate is the sum of surface and bulk scattering rates. Therefore, the mobility μ will be determined from the mobility μ_b existent in the absence of surface scattering in the bulk material and from the mobility μs which would be present in that sample in the absence of bulk scattering

$$\frac{1}{\mu} = \frac{1}{\mu_b} + \frac{1}{\mu_s}. \tag{3.17}$$

The quantum $1/f$ fluctuations will therefore satisfy the relation

$$\frac{\delta\mu}{\mu^2} = \frac{\delta\mu_b}{\mu_b^2} + \frac{\delta\mu_s}{\mu_s^2}. \tag{3.18}$$

Consequently, the CQ$1/f$E spectral density $S_{\delta\mu/\mu}(f) \equiv <(\delta\mu/\mu)^2>_f$ satisfies the relation

$$S_{\frac{\delta\mu}{\mu}} = \left(\frac{\mu^2}{\mu_b^2}\right)\left\langle\left(\frac{\delta\mu_b}{\mu_b}\right)^2\right\rangle_f + \left(\frac{\mu^2}{\mu_s^2}\right)\left\langle\left(\frac{\delta\mu_s}{\mu_s}\right)^2\right\rangle_f. \tag{3.19}$$

For the quantum $1/f$ noise in the bulk mobility we write

$$\left\langle\left(\frac{\delta\mu_b}{\mu_b}\right)^2\right\rangle_f = \left(\frac{4\alpha}{3\pi Nf}\right)\left\langle\left(\frac{\hbar\Delta k}{mc}\right)^2\right\rangle = \left(\frac{4\alpha}{3\pi Nf}\right)\left(\frac{0.75\,h}{amc}\right)^2 \tag{3.20}$$

where m is the effective mass of the carriers, and the effective Δk was taken to be 0.75 G. Here G is the smallest reciprocal lattice vector $2\pi/a$, where a is the lattice constant and

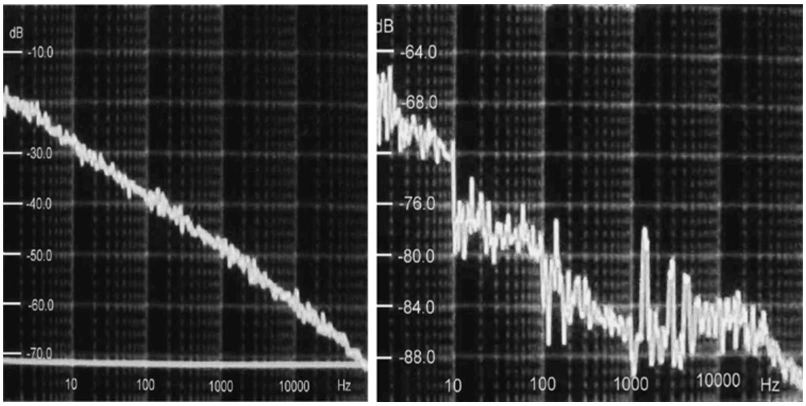

Fig. 4. Typical l/f noise spectrum of the HFET channel, with the much lower background measured by us, on the right.

$h = 2\pi\hbar$ Finally, $\alpha = e^2/\hbar c$ is Sommerfeld's fine structure constant and N is the number of carriers in the sample.

The conventional Q$1/f$E in the surface-scattering-limited mobility μ_s is obtained from (3.16) by substituting

$$\left(\frac{\Delta \mathbf{v}}{c}\right)^2 = \frac{6kT^2}{mc} + \frac{2eV_o}{m}. \tag{3.21}$$

This yields

$$\left\langle \left(\frac{\delta\mu_s}{\mu_s}\right)^2 \right\rangle_f = \left(\frac{4\alpha}{3\pi N f}\right)\left[\frac{6kT^2}{mc} + \frac{2eV_o{}^2}{mc}\right] \tag{3.22}$$

where e is to be replaced by $-e$, and m by m' the case of inversion, m and m' being the effective masses of the carriers.

The final expression for the resulting power spectrum of quantum $1/f$ mobility fluctuation is thus

$$S_{\frac{\delta\mu}{\mu}} \equiv \frac{\alpha_{\text{conv}}}{Nf} = \left(\frac{4\alpha}{3\pi N f c^2}\right) \times \left[\left(\frac{\mu}{\mu_b}\right)^2 \left(\frac{0.75h}{am}\right)^2 + \left(\frac{\mu}{\mu_s}\right)^2 \left(\frac{6kT}{m} + \frac{2eV_o}{m}\right)\right]. \tag{3.23}$$

In this expression, the quantity in round brackets in the second term on the right hand side is always smaller than the corresponding round bracket present in the first term, corresponding to lattice scattering, and characteristic for the bulk material. However, the relative contribution of the two terms on the right-hand side depends on the sample thickness. For a given sample, this second term can be further reduced by treating the surface in order to obtain a depletion layer (with a small $V_o < 0$ for n-type material).

Influence of Dislocations Arising From Bending Deformation: Uniform bending with a radius of curvature R will generate a surface density of dislocations of $\rho = 1/aR$ and an additional volume density of defects $n_{\text{dis}} = 1/a^2R$ in the given ultrathin sample. Assuming we know the measured mobility μ_o of the given sample before bending, the theoretical mobility $\mu_l = \mu_{\text{lattice}}$ of the ideal sample with no defects (limited by phonon scattering, intervalley and Umklapp only) and the concentration of defects n_{odef} in the given sample before bending, we can derive for the quantum $1/f$ noise spectral density of fractional fluctuations expected in the bent ultrathin sample the approximate formula

$$S_{\frac{\delta\mu}{\mu}} = \left\{\frac{(\mu_o^2)}{[(1+r)\mu_l - r\mu_o]^2}\right\} S^{\text{latt}}_{\frac{\delta\mu}{\mu}}(f) \tag{3.24}$$

in which $r = n_{\text{dis}}/n_{\text{odef}}$, and $S^{\text{latt}}_{\delta\mu/\mu}(f)$ is the theoretical quantum $1/f$ spectral density affecting μ_l in an ideal sample with no defects, being caused by phonon scattering, intervalley and Umklapp only. This formula is obtained by neglecting the quantum $1/f$ noise of defect scattering (both ionized or neutral, both impurity defects and lattice defects) compared to the much larger quantum $1/f$ noise of lattice scattering, including phonon scattering, intervalley and Umklapp in the ideal lattice.

If a lattice constant of $a = 1$ Å and a bending radius of curvature $R = 10$ cm are considered, the resulting dislocation densities of $\rho = 10^7$ cm^{-2} and $n_{\text{dis}} = 10^{15}$ cm^{-3} have to be compared with the preexisting concentration of defects n_{odef}. Assuming $n_{\text{odef}} = 10^{16}$ cm^{-3}, we obtain $r = 0.1$. The resulting correction is a small reduction in the expected noise. However, this calculation neglects all current-redistribution effects which result from a nonuniform distribution of dislocations introduced by bending. It also neglects the effect of the decreased lifetime of the carriers in bent ultrathin ICs, in particular on the junction devices or on other unwanted junctions present in the IC. All these effects result in increased conventional quantum $1/f$ noise. The increased nonuniformity of the current distribution also results in an increase of the coherent quantum $1/f$ effect present in the larger samples, as we see in the next section.

E. *Quantum $1/f$ Effect in Spin-Polarized Transport and Spintronic Devices*

The spin-polarized leakage current passing through a closed spin-valve is caused by electron spin-flip processes. The rate of these processes controls the rate of current flow. Without a spin-flip, the electron cannot go through the valve. The electronic spin-flip rate is affected by quantum $1/f$ noise because the spin-flip emits bremsstrahlung just like any sudden current change $\Delta J = (e/L)\Delta v$ would do. The conventional quantum $1/f$ effect (Q$1/f$E) in any rate Γ

or cross section σ is a macroscopic quantum phenomenon described by the quantum $1/f$ engineering formula

$$S_{\frac{\delta\Gamma}{\Gamma}}(f) = S_{\frac{\delta\sigma}{\sigma}}(f) = S_{\frac{\delta j}{j}}(f) = \left(\frac{4\alpha}{3\pi f N}\right)\left(\frac{\Delta \mathbf{v}}{c}\right)^2. \tag{3.25}$$

Here $S_{\delta\Gamma/\Gamma}(f)$ is the spectral density of fractional fluctuations in current $\delta j/j$ in scattering or recombination cross section $\delta\sigma/\sigma$ or in any other process rate $\delta\Gamma/\Gamma$. $\alpha = e^2/\hbar c = 1/137$ is Sommerfeld's fine structure constant, a magic number of our world depending only on Planck's constant $\hbar$, the charge of the electron e, and the speed of light in vacuum c. $A = 2(\Delta v/c)^2/3\pi$ is essentially the square of the vector velocity change Δv of the scattered particles in the scattering process whose fluctuations we are considering, in units of c. Finally, $N = LN'$ is the number of particles used to define the notion of current j, of cross section σ, or of process rate Γ.

This applies to the *quantum $1/f$ fluctuations of the electronic spin-flip rate*, or *decoherence rate*, as mentioned above. Decoherence is caused by the elementary spin-flip of a nucleus due to its various interactions. The particular nature of these is not important here, due to the well-known quantum $1/f$ universality that characterizes all IR divergence phenomena. The rate of this process has quantum fluctuations according to (3.25). It reduces the total magnetic moment M of the sample by the magnetic moment $\mu = e\hbar/2\,mc = 1$ Bohr magneton of a single electron spin undergoing a change of one $\hbar$ in its spin projection. The current change $e\Delta v$ causing bremsstrahlung is here $(\Delta\,\dot{\mathbf{M}})/e$, the change in the rate of demagnetization caused by the emission of an energy quantum, a photon. This yields

$$S_{\frac{\delta\Gamma}{\Gamma}}(f) = \frac{4\alpha\left\langle(\Delta v)^2\right\rangle}{3\pi f c^2} = \frac{4\alpha\left\langle(\Delta\,\dot{\mathbf{M}})^2\right\rangle}{3\pi f e^2 c^2}. \tag{3.26}$$

Let N be the number of elementary magnetic dipoles $\mu = e\hbar/2mc$ present in the magnetic induction field B and aligned parallel to it. Applying a variation $\Delta N = 2$ for a spin reversal, we get

$$\frac{\Delta n}{n} = \frac{\Delta N}{N} = \frac{|\Delta\,\dot{\mathbf{M}}\,|}{|\,\dot{\mathbf{M}}\,|} \quad \text{or}$$

$$\left\langle(\Delta\,\dot{\mathbf{M}})^2\right\rangle = \frac{\left\langle(\dot{\mathbf{M}})^2\right\rangle}{N^2} = 8\,\mu^4 H^2 N^2/\hbar^2 \tag{3.27}$$

where we used Larmor's theorem $\dot{\mathbf{M}} = \omega \times \mathbf{M}$, with $\omega = N\mu\mathbf{H}/\hbar$. Substituting $\Delta\,\dot{\mathbf{M}}$ into (3.26), we get

$$S_{\frac{\delta j}{j}} = \Gamma^{-2} S_\Gamma(f) = \frac{32\alpha\mu^4 H^2 N^2}{3\pi f e^2 c^2 \hbar^2}. \tag{3.28}$$

This is the spectral density of fractional quantum $1/f$ fluctuations in the rate Γ of spin-flip or decoherence (electrodynamical Q1/fE only). This spectral density of fractional fluctuations will affect the spin-polarized leakage current j through the device. There is also shot noise $S_{\delta j/j} = 2ej$.

F. Phase Noise in RTDs and in Oscillators Based on Them, up to Terahertz (THz) Frequencies

For imaging and remote sensing applications, the phase noise of the THz generator must be minimized. This can be done as part of the optimization process on the basis of a properly chosen figure of merit. For this, this paper provides an analytical phase noise expression as a function of the device parameters and operation point. The quantum $1/f$ theory is used to calculate from first principles the $1/f$ noise present in the device parameters and in the resulting system frequency from RTDs, super-electronic lattice devices (SLEDs), Gunn devices (TEDs), and transit time diodes. In general, quantum $1/f$ fluctuations in the dissipative elements lead to a Q^{-4} dependence of the spectral density of fractional frequency fluctuations and of the corresponding phase noise, where Q is the quality factor.

RTDs have been proposed as generators of THz oscillations and radiation. They consist of two potential barriers enclosing a quantum well. Electrons penetrating the potential barriers by tunneling are controlled by the quasi-stationary energy levels defined by the penetrating the potential barriers by tunneling are controlled by the quasi-stationary energy levels defined by the potential well. If their energy is close to the first energy level in the well, resonance occurs, and a peak IP of the current through the diode occurs. This corresponds to an applied bias voltage VP. If, however, the applied voltage increases further, only a negligibly small nonresonant current trickle remains at the voltage $V = V_v$ and a broad valley is observed in the I/V characteristic. Scattering processes that reduce the energy of the carriers to a value close to eVP will always be present, generating a finite current minimum I_V at V_v. Between V_P and V_v, there is a negative differential conductance

$$G = -\frac{(I_P - I_V)}{(V_v - V_P)} \tag{3.29}$$

on the I/V curve that is used to generate oscillations. The $1/f$ noise in I_V is given by (2.2) with

$$\left(\frac{\Delta v}{c}\right)^2 = \frac{2eV_V}{m}. \tag{3.30}$$

Taking, for instance, $V_P = 0.4\,V$, $I_P = 2.5\,10^8$ A/m^2, $V_v = 0.6$ V, $I_V = 4\,10^7$ A/m^2, we obtain with $m_{\text{eff}} = 0.068\,m_o$

$$N I_V^{-2} S_{Iv}(f) = \frac{2\alpha A}{f} = \frac{7.4}{0.068\,10^{-9}} = 1.3\,10^{-7}. \tag{3.31}$$

N is given by

$$N = \frac{\tau I_V}{e} \tag{3.32}$$

where τ is the lifetime of the carriers. With a cross-sectional area of 10^{-6} cm^2 and $\tau = 10^{-10}$, we obtain $N = 2.5 \cdot 10^6$.

Finally, the quantum $1/f$ frequency fluctuations can be obtained from the formula

$$S_{\frac{\delta\omega}{\omega}} = \left(\frac{1}{4Q^4}\right) S_{\frac{\delta G}{G}} \quad (3.33)$$

which is derived below. This finally yields with (3.25)

$$S_{\frac{\delta\omega}{\omega}} = \left(\frac{1}{4Q^4}\right)\left(\frac{4\alpha}{3\pi}\right)\left(\frac{2eV_V}{mc^2}\right) \quad (3.34)$$

for the fractional frequency fluctuation spectrum exhibited by the RTD if included in an RF circuit of quality factor Q.

G. *Frequency and Phase Fluctuations From $1/f$ Noise in Dissipation*

Resonant systems can be described as a harmonic oscillator with losses

$$\frac{dx}{dt} + \frac{\gamma dx}{dt} + \omega_o^2 x = F(t). \quad (3.35)$$

The quantum $1/f$ fluctuations are present in the loss coefficient γ. They are given by an expression of the form

$$S_{\frac{\delta\gamma}{\gamma}}(f) = \frac{\Lambda}{f} \quad (3.36)$$

where Λ is a quantum $1/f$ coefficient characterizing the elementary loss process.

The resonance frequency is given by

$$\omega_r^2 = \omega_o^2 + \gamma^2. \quad (3.37)$$

The quantum $1/f$ fluctuations in the resonance frequency are given by $\omega_r \delta\omega_r = -2\gamma\delta\gamma$, or

$$\frac{\delta\omega_r}{\omega_r} = -2\left(\frac{\gamma}{\omega_r}\right)^2 \frac{\delta\gamma}{\gamma} = -\left(\frac{1}{2Q^2}\right)\left(\frac{\delta\gamma}{\gamma}\right) \quad (3.38)$$

where $Q = \omega_r/2\gamma$ is the quality factor. Squaring, averaging, and particularizing (3.16) for the unit frequency interval, we obtain the Q^{-4} law

$$S_\omega(f) = \left\langle \left(\frac{\delta\omega_r}{\omega_r}\right)^2 \right\rangle_f = \left(\frac{1}{4Q^4}\right) \left\langle \left(\frac{\delta\gamma}{\gamma}\right)^2 \right\rangle_f = \frac{\Lambda}{4fQ^4} \quad (3.39)$$

where y is the fractional frequency fluctuation $\delta\omega_r/\omega_r$. This law is also applicable to quartz resonators, where it was first introduced [3] in 1978. The phase noise is obtained from

$$S_\phi(f) = \left(\frac{\omega_r}{2\pi f}\right)^2 S_y(f) \quad \text{or} \quad L(f) = \left(\frac{1}{2}\right) S_\phi(f) \quad (3.40)$$

the latter being a two-sided power spectrum often given in decibels. The examples in the last two sections show how the phase noise is to be found in other solid-state sources of THz radiation.

IV. Quantum $1/f$ Phase Noise in Resonators, Resonant Sensors, and Oscillators

Piezoelectric sensors used for the detection of chemical agents and for electronic nose instruments are based on BAW and SAW resonators. They are also useful in the detection of biological agents and can be specific, particularly if the sensitive surface is activated with the right antigen.

The BAW resonators are used for instance in the quartz crystal microbalance (QCM). This is usually a polymer-coated resonating quartz disk, a few millimeter in diameter, with smaller diameter metal electrodes on each side and with quality factor Q. The resonance frequency is usually in the 10–30-MHz range. Absorption of gas molecules with mass δm on the surface of the polymer coating gets detected by a reduction of the resonance frequency of the quartz disk, subject also to fundamental quantum $1/f$ frequency fluctuations. The quantum $1/f$ limit of detection is given by the quantum $1/f$ formula for quartz resonators. To optimize the device, we must avoid closeness of the crystal volume to the phonon coherence length which corresponds to the maximum error and minimal sensitivity situation. Differential measurements that include a reference resonator without polymer coating can effectively eliminate temperature fluctuations, power supply instability, etc. Adsorbed masses below the pg range can be detected.

Similarly, SAW resonators are used at about ten times higher frequencies in small sensors that operate best with sizes larger than the phonon coherence length. The discussion is similar, but applied to the surface and surface waves.

A. *Introduction: Application of the Conventional Quantum $1/f$ Effect, a New Aspect of Quantum Mechanics*

According to the quantum $1/f$ effect, quantum-mechanical cross sections σ_o and process rates Γ_o are considered to be just the expectation values of the physical quantities σ and Γ that also contain the quantum $1/f$ fluctuations. Therefore

$$S_{\frac{\delta\sigma}{\sigma}}(f) = S_{\frac{\delta\Gamma}{\Gamma}}(f) = \left(\frac{4\alpha}{3\pi f}\right)\left(\frac{\Delta v}{c}\right)^2 = \frac{4\alpha(\Delta\,\dot{\mathbf{P}})^2}{3\pi f e^2 c^2}. \quad (4.1)$$

Here $\alpha = (1/4\pi\varepsilon_o)(2\pi e^2/hc) = 1/137$ is Sommerfeld's fine structure constant, a dimensionless universal constant constructed from Planck's constant, the charge e of the electron, and the speed of light c.

Phonon scattering in the resonator crystal was long suspected to limit the short- and medium-term frequency stability in all crystal resonators [56]. Phonon scattering can occur on other phonons (particularly at higher temperatures) or on crystal defects (favored by default at low temperatures). In both cases, this process is shown to yield a $1/f$ spectrum of resonator frequency fluctuations through the conventional quantum $1/f$ effect. As was first shown on this basis with the help of a simple harmonic oscillator model [26], BAW and SAW quartz resonators ought to have a Q^{-4} dependence of their FM power spectrum. This has been experimentally verified by Gagnepain and Uebersfeld for BAW resonators [58] when they noticed their $1/Q^{4.4}$ law, and by Parker for the SAW case [59], [79]. Although the quantum $1/f$ effect provided the historical basis for the derivation of the Q^{-4} law [57] as being caused by fluctuations in the dissipation rate of the quartz resonator, the exact mechanism through which the quantum $1/f$ effect modulates the dissipation rate remained unknown from 1978 to 1991.

Finally, the bridge directly connecting $1/f$ noise in frequency standards to the quantum $1/f$ effect was discovered [60]–[62], yielding simple quantum $1/f$ engineering formulas. *In this section, this thorough understanding and knowledge is used to calculate the fundamental sensitivity limits of quartz resonator sensors used for the detection of biological and chemical agents.*

Here is how it works. The rate Γ of phononinteractions which remove phonons from the main quartz sensor's resonator mode is modulated by the quantum $1/f$ effect, therefore exhibiting observable (macroscopic) quantum fluctuations, while its expectation value remains constant. Indeed, whenever a phonon is removed from the main resonator mode, the time derivative of the polarization vector of the quartz crystal $d\mathbf{P}/dt = \dot{\mathbf{P}}$ is suddenly affected, suffering a step-like modification as a function of time. From Maxwell's equations, we know, however, that $\dot{\mathbf{P}}$ is added to the current J and that such a modification of the current causes radiation. Solving Maxwell's equations we find that as a result of the phonon removal, there is a constant energy of $(1/4\pi\varepsilon_o)^4(\Delta\, \dot{\mathbf{P}})^2/3c^3$ radiated away per unit frequency, interval, i.e., per hertz at any frequency f. Dividing this result by the energy of a photon hf, we find that there is thus a probability of $2\alpha(\Delta\, \dot{\mathbf{P}})^2/3\pi f e^2 c^2$ for the emission (radiation) of a bremsstrahlung photon of frequency f. SI units are used here, while Gaussian units were used in [62].

Since there is a probability of $2\alpha(\Delta\, \dot{\mathbf{P}})^2/3\pi f e^2 c^2 \ll 1$ for the emission of a bremsstrahlung photon of frequency f, the quartz crystal suffers a reaction, or a recoil in its quantum state. This causes the phononemission rate Γ to perform quantum oscillations with frequency f and with two-sided spectral density S' of fractional fluctuations given by the same expression, $S'\delta\Gamma/\Gamma(f) = 2\alpha(\Delta\, \dot{\mathbf{P}})^2/3\pi f e^2 c^2$. This is here the expression of the quantum $1/f$ effect. The one-sided spectrum is thus, as was mentioned in the last form of (4.1)

$$S_{\frac{\delta\Gamma}{\Gamma}}(f) = \frac{4\alpha(\Delta\, \dot{\mathbf{P}})^2}{3\pi f e^2 c^2}. \tag{4.2}$$

This means that any radiation caused or implied by a quantum transition from one state to another comes with a price. It reacts back on the system, causing the rate of that transition to be modulated by exhibiting observable macroscopic quantum fluctuations. These have a spectral density of fractional rate fluctuations identical to the photon-emission probability accompanying the transition considered. No knowledge of quantum mechanics is therefore needed in order to apply the quantum $1/f$ effect. One has to divide the energy radiated by the energy hf of one photon of frequency f. This is based just the reality of Planck's constant h and Planck's relation between photon energy and frequency. Knowledge of electrodynamics is needed, however, in order to calculate the energy radiated in a transition.

The reader interested in a basic understanding of the quantum $1/f$ effect will find a most accessible description in [63, pp. 8–9]. That description considers scattering of electrons as an example of transition which emits radiation and suffers a quantum $1/f$ modulation of its rate, rather than considering scattering of phonons, which, as we believe, is most important in crystal resonators. All that is involved in that derivation is the notion of DeBroglie wave associated to a particle, or the notion of wave function. Old quantum mechanics notions are thus sufficient for a basic understanding of the recoil, or energy-loss mechanism, of the quantum $1/f$ effect (Q$1/f$E). For a practical application of the Q$1/f$E, however, classical physics is sufficient.

B. *Quartz Crystal Microbalances*

Piezoelectric sensors are useful for the following purposes.

- Detection of chemical agents and for electronic nose instruments; based on BAW and SAW resonators.
- Detection of biological agents and can be specific, particularly if the sensitive surface is activated through deposition of a layer of the right specific antigen, that "attracts" a certain bacterium, microbe, or virus. The antigens are produced by organisms in order to fight, or bind, the pathogenic agents mentioned here.

Piezoelectric sensors are of two kinds: BAW resonator based and SAW resonator based. The former are used, for instance, in the QCM. This is usually a polymer-coated resonating quartz disk, a few millimeter in diameter, with smaller diameter metal electrodes on each side and with quality factor Q. Their resonance frequency is usually in the 10–30-MHz range, and ten times higher for SAWs.

These sensors are based on the adsorption of many gas molecules (with total mass δm) on the surface of the polymer coating. This gets detected by a reduction

$$y = \frac{\delta\nu}{\nu} = -\frac{\kappa\delta m}{m} \tag{4.3}$$

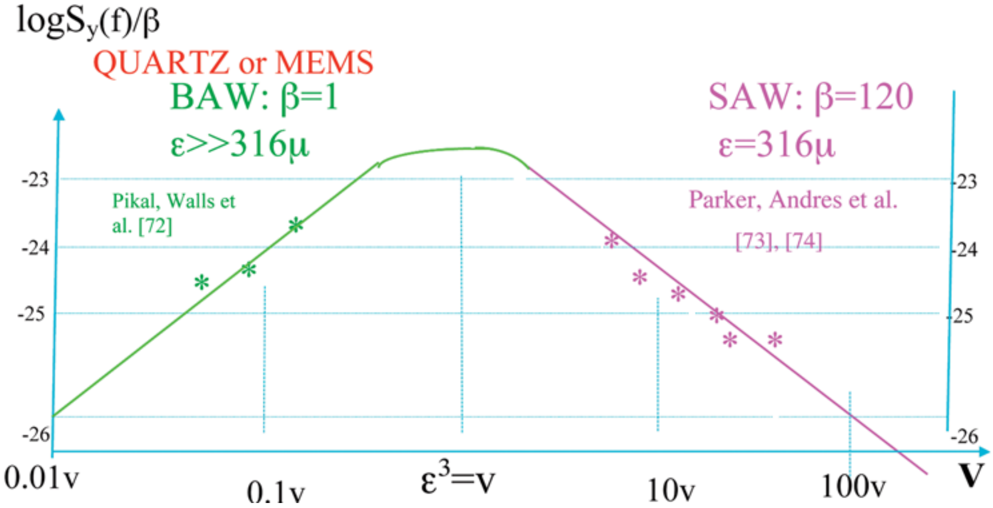

Fig. 5. Quantum $1/f$ noise in BAW and SAW resonators yields bio/chem. sensitivity limit.

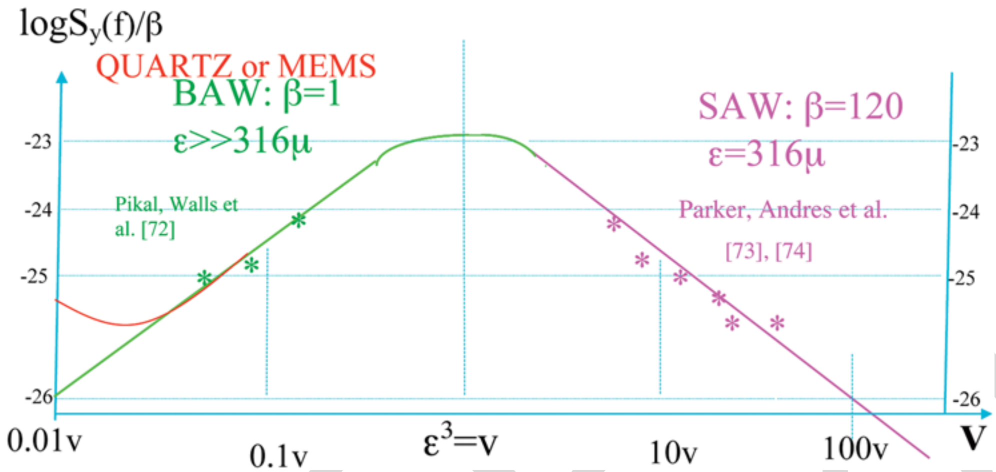

Fig. 6. Total FM noise in Si MEMS and quartz BAW and SAW resonators; the red line adds the classical white noise at small volumes.

of the resonance frequency of the quartz disk. However, the latter is also subject to fundamental frequency fluctuations. Here κ is a constant of proportionality. The quantum $1/f$ limit of detection is given by

$$\kappa^2 S_{\frac{\delta m}{m}}(f) = S_y(f) \tag{4.4}$$

where $S_y(f)$ is given by formulas [57], [60]–[63]

$$S_y(f) = \frac{\beta' V}{f Q^4}, \quad \text{for} \quad V \leq \varepsilon^3 \tag{4.5}$$

and

$$S(f) = \frac{\beta' \varepsilon}{f V Q^4}, \quad \text{for} \quad V \geq \varepsilon^3 \tag{4.6}$$

as we show below. Here ε^3 is the phonon coherence volume, first introduced empirically by Parker *et al.* as a noise coherence volume.

To optimize the device we must avoid closeness of V *with* ε, *which corresponds to the maximum error and minimal sensitivity situation*. (See the central region in Fig. 5.)

To reduce the measurement errors, one uses differential measurements, that include a reference resonator without polymer coating and subtract its frequency changes. This can effectively eliminate the destabilizing effect of temperature fluctuations, power supply instability, etc. This way, adsorbed masses below the $pg = 10^{12}$ g range can be detected.

Calculation of the Quantum $1/f$ *Sensitivity Limit:* With $\langle\omega\rangle = 10^3/s$ being the average circular frequency of a thermal phonon interacting with phonons in the main resonator mode, with $n = kT/\langle\omega\rangle\hbar$ being the average number of phonons in that typical thermal phonon mode, and with $T = 300$ K, we obtain approximately for the quantum $1/f$ noise coefficient β' in (5), (6) (see below)***[AU: Please provide correct equation references]***

$$\beta' = \frac{\left(\frac{N}{V}\right)\alpha\hbar\langle\omega\rangle}{12 n\pi g^2 m c^2} = \frac{\left(\frac{1}{137}\right)(10^{-27}\ 10^8)2}{12kT\pi 10^{-27} 9\cdot 10^{20}} = 1. \tag{4.7}$$

For $V < \varepsilon^3$, this is in good agreement with the known data for quartz resonators of very high Q, as experimental results obtained by Walls *et al.*, Parker *et al.*, Vig *et al.*, as well as other research groups indicate. Here m is the reduced mass of the elementary oscillating dipoles, N their number in the quartz resonator volume, and g a polarization constant of the order of the unity.

C. SAW Sensors

The same way, SAW resonators are used at about higher frequencies in sensors that operate in the $V > \varepsilon^3$ regime. The discussion is similar, but applied to the surface and surface acoustic waves. In that case, the coherence length of the phonons is smaller than the crystal size, and therefore we expect several incoherent noise contributions from various regions of the crystal.

Spatial Incoherence of Phonon Loss Rate Fluctuations in Low and Intermediate Q Resonators: Considering the $\nu = V/\varepsilon^3$ independently fluctuating regions similar, we replace (4.1) by

$$S_{\frac{\delta\Gamma}{\Gamma}}(f) = \sum_{i=1}^{\nu} \left\langle \left(\frac{\delta\Gamma_i}{\Gamma}\right)^2 \right\rangle_f = \nu^{-1} \left\langle \left(\frac{\delta\Gamma_i}{\Gamma_i}\right)^2 \right\rangle_f = \frac{4\alpha(\Delta\dot{\mathbf{P}}_\mathbf{i})^2}{3\pi f \nu e^2 c^2}. \tag{4.8}$$

Here we assumed that $\Gamma = \nu\Gamma_i$ and that $< (\delta\Gamma_i/\Gamma_i)^2 >_f = \nu S_{\delta\Gamma/\Gamma}(f)$ is independent of i. With $\nu = V/\varepsilon$ we finally obtain

$$S_{\frac{\delta\Gamma}{\Gamma}}(f) = \frac{4\alpha\varepsilon^3(\Delta\dot{\mathbf{P}}_\mathbf{i})^2}{3\pi f V e^2 c^2} = \frac{4\alpha\varepsilon^2(\Delta\dot{\mathbf{P}}_\mathbf{i})^2}{3\pi f A e^2 c^2}. \tag{4.9}$$

Note that the phonon mean free path is about 40 Å for bulk wave phonons in quartz at room temperature and 500 Å at liquid nitrogen temperatures. This approximates the phonon coherence length ε very well. For SAW phonons the corresponding coherence length values may be four times lower due to the smaller velocity of the surface wave and due to its stronger scattering. The wave is localized within about two coherence lengths ε from the surface. Therefore, in the incoherent regime, $V = 2\varepsilon A$ is a good approximation. Consequently, we expect an increase of $S_{\delta\omega/\omega}(f)$ proportional with $1/A$ when the resonant area A is decreased, down to very small areas of the order of ε^2.

Coherent Case of High-Q Resonators: From (4.2) we obtain

$$S_{\frac{\delta\Gamma}{\Gamma}}(f) = \frac{4\alpha(\Delta\dot{\mathbf{P}})^2}{3\pi f e^2 c^2}. \tag{4.10}$$

The vibrational energy of the crystal can be written in the form

$$W = n^{\hbar}\langle\omega\rangle = 2\left(\frac{\text{nm}}{2}\right)\left(\frac{dx}{dt}\right)^2 \tag{4.11}$$

$$= \left(\frac{\text{nm}}{e^2}\right)\left(\frac{edx}{dt}\right)^2 = \left(\frac{m}{Ne^2}\right)\varepsilon^2(\dot{\mathbf{P}}_\mathbf{i})^2. \tag{4.12}$$

The factor two includes the potential energy contribution. Here m is the reduced mass of the elementary oscillating dipoles, e their charge, g a polarization constant of the order of the unity, and N their number in the resonator. Applying a variation $\Delta n = 1$, we get

$$\frac{\Delta n}{n} = \frac{2|\Delta\dot{\mathbf{P}}\,|}{|(\dot{\mathbf{P}}\,|}, \text{ or } \Delta\dot{\mathbf{P}} = \frac{\dot{\mathbf{P}}}{2n}. \tag{4.13}$$

Solving (4.12) for $\dot{\mathbf{P}}$ and substituting into (4.13), we obtain

$$|\Delta\dot{\mathbf{P}}\,| = \left(\frac{N\hbar\langle\omega\rangle}{n}\right)^{\frac{1}{2}}\left(\frac{e}{2g}\right). \tag{4.14}$$

Substituting $\Delta\ \dot{\mathbf{P}}$

$$\Gamma^{-2}S_\Gamma(f) = \frac{N\alpha\hbar\langle\omega\rangle}{3n\pi mc^2 f g^2} \equiv \frac{\Lambda}{f}. \tag{4.15}$$

Using the harmonic oscillator relation

$$\omega^2 = \omega_o^2 - 2\Gamma^2, \quad \omega\delta\omega = -2\Gamma\delta\Gamma \tag{4.16}$$

between resonance frequency ω and dissipation Γ, we obtain

$$S_{\frac{\delta\omega}{\omega}}(f) = \left(\frac{1}{4Q^4}\right)S_{\frac{\delta\gamma}{\gamma}}(f) = \left(\frac{1}{4Q^4}\right)\left(\frac{\Lambda}{f}\right) = \frac{N\alpha\hbar\langle\omega\rangle}{12n\pi mc^2 f g^2 Q^4} \tag{4.17}$$

$$S(f) = \frac{\beta' V}{fQ^4}, \text{ for } V \leq \varepsilon^3 \tag{4.18}$$

and

$$S(f) = \frac{\beta'\varepsilon^6}{fVQ^4}, \text{ for } V \geq \varepsilon^3 \tag{4.19}$$

as was stated in (4.5) and (4.6) above. Here, with an intermediary value $\langle\omega\rangle = 10^8/s$, with $n = kT/\hbar\langle\omega\rangle$, $T = 300$ K and $kT = 4 \cdot 10^{-21}\ J$, we get

$$\beta' = \frac{\left(\frac{N}{V}\right)\alpha\hbar\langle\omega\rangle}{12n\pi g^2 mc^2} = \frac{10^{22}\left(\frac{1}{137}\right)(10^{-27}10^8)^2}{12kT\pi 10^{-27}\ 9\ 10^{20}} = 1. \tag{4.20}$$

as stated above in (4.7) (the thermal $\langle\omega\rangle$ can be calculated rigorously.

The Case of Defect Scattering: A Two-Phonon Process: A phonon from the main resonator mode scatters on a defect and a phonon of comparable frequency emerges into another mode with much smaller phonon occupation number $n_\omega = kT/\hbar\omega$. In this case, we have to replace $\langle\omega\rangle$ by ω and $n_{\langle\omega\rangle}$ with n_ω, which gives a β-value which is $(\langle\omega\rangle/\omega)^2$ smaller, i.e., 10^4–10^6 times smaller.

The General Case: With $\Gamma = \Gamma' + \Gamma''$, we obtain for the combined phonon and defect scattering case, in general

$$\beta = \frac{\beta'\left[\Gamma'^2 + \left(\frac{\omega}{\langle\omega\rangle}\right)^2 \Gamma''^2\right]}{\Gamma^2}. \tag{4.21}$$

Although the defect scattering term is small at room temperature, it may become dominant at low temperatures, when the phonon scattering rate Γ' becomes much smaller than the defect scattering rate Γ''.

Since the $1/f$ noise level depends on the active volume, in the coherent regime one should use the lowest overtone and smallest diameter consistent with other circuit parameters. In the incoherent (low Q) case, the opposite should be considered.

D. Silicon MEMS Resonator Sensors

The classical forms of noise present in the frequency of MEMS resonators, have been recently investigated and described in detail [64]. This section extends this investigation to $1/f$ noise. That is of fundamental nature in MEMS resonators, and is given by the universal quantum $1/f$ effect, with some similarities to the case of quartz resonators. When the environmental fluctuations are reduced, e.g., by temperature stabilization, elimination of molecular adsorption, etc., the fundamental limitation introduced by the quantum $1/f$ effect becomes visible as a flicker floor in the time-domain noise representation. Being ultimately based on Heisenberg's uncertainty relations, this effect defines the quantum limit achievable at low frequencies, when the classical sources of noise have been sufficiently reduced.

The quantum $1/f$ effect manifests itself in MEMS resonators through conventional quantum $1/f$ noise. This is a quantum fluctuation present in the quantum mechanical notion of "physical cross section" σ and "physical process rate" Γ, caused by the reaction of the electromagnetic field on the charged particle that emitted it, or in general, on the system that emitted it. It is given by the spectral density of fractional fluctuations, as in (3.25)

$$S_{\frac{\delta\sigma}{\sigma}}(f) = S_{\frac{\delta\Gamma}{\Gamma}}(f) = \left(\frac{4\alpha}{3\pi f}\right)\left(\frac{\Delta v}{c}\right)^2 \tag{4.22}$$

where Δ_v is the velocity vector change of the current carriers of charge e. As shown in the case of BAW and SAW quartz resonators, of ferroelectrics, and of antennas, the rate Γ of interest for the calculation of $1/f$ resonance frequency fluctuations in Si MEMS is the rate of phonon removal from the main mechanical oscillation mode of the oscillating bar. As in the above-mentioned cases, our mechanism of quantum $1/f$ noise generation is based on bremsstrahlung from electric or magnetic dipoles, rather than from scattering of individual carriers.

The MEMS resonators are shaped as a bar of micro- or nanometric dimensions incased (fixed) at both ends, and subject to bending strain. They are driven by an ac current I flowing in a very thin straight wire attached along the bar, in the presence of a strong constant magnetic field $\mathbf{B}$, perpendicular to it. Alternatively, they could be driven electrostatically, or capacitively, by using the wire, or a metallic thin sheet deposited along that side of the bar, as one of the two "plates" of a capacitor. An ac voltage would then be applied to the capacitor at the resonance frequency. Note that in fact there is nothing resembling a bar in the actual MEMS devices. In practice there are comb resonators, "free-free" resonators, and probably others too (J. Vig., private communication). Details are found, e.g., in Nguyen's publications [65]–[70]. For simplicity, we continue to refer here to the idealized case of a bar, using effective dimensions that correspond to the actual geometry at hand.

The approach developed for the case of resonators based on quartz and other piezoelectric substances cannot be applied to Si MEMS resonators, because silicon is not piezoelectric. It could only be applied to piezoelectric MEMS resonators, using, for instance, quartz. We therefore develop a new approach in this paper, applicable to the new, driven MEMS resonators. We consider below both the case of magnetic excitation and the capacitive case.

Magnetic Excitation of a Resonant Silicon MEMS Bar: The elementary act of dissipation is the absorption of one phonon from the main resonator mode. This can happen either through three photon processes, dominant at higher temperatures, or through two processes, dominant at low temperatures, in the presence of crystal defects of various types. In both cases, this elementary act has a spontaneous "bremsstrahlung photon emission (probability) amplitude" associated with it, because it causes a sudden reduction $\Delta\,\dot{\mathbf{m}}$ of the rate $d\mathbf{m}/dt \equiv \dot{\mathbf{m}}$ of change of the magnetic dipole moment of the system. The system is defined here to include the current carrying circuit, the applied magnetic field $\mathbf{B}$ with the agency generating it, plus the oscillating bar, i.e., the MEMS. The rate $\dot{\mathbf{m}}$ of change of the magnetic dipole moment of the system is caused by bending oscillations of the bar with the current-carrying wire attached to its side, cutting the lines of force of $\mathbf{B}$ while it moves.

The conventional quantum $1/f$ noise in the rate of dissipation Γ is obtained in the CGS Gaussian system by simply replacing the current change $e\Delta\mathbf{v}$ with $\Delta\,\dot{\mathbf{m}}$

$$S_{\frac{\delta\Gamma}{\Gamma}}(f) = \left(\frac{4\alpha}{3\pi f}\right)\left(\frac{\Delta\dot{\mathbf{m}}}{ec}\right)^2. \tag{4.23}$$

To calculate the change $\Delta\,\dot{\mathbf{m}}$, we note that $(\dot{\mathbf{m}})^2$ is proportional to the transversal vibration speed of the bar and to the total mechanical energy $W = (n + 1/2)\hbar\omega$ in the main oscillation mode of the resonator

$$\left(n+\frac{1}{2}\right)\hbar\omega=\frac{\kappa(\dot{\mathbf{m}})^2}{2}. \tag{4.24}$$

Here κ is a coefficient of proportionality easy to calculate. When a phonon is removed from the main MEMS resonator mode, the energy in (4.24) is reduced by the amount

$$\hbar\omega=\kappa\,\dot{\mathbf{m}}\ \Delta\dot{\mathbf{m}}\,. \tag{4.25}$$

This yields

$$(\Delta\dot{\mathbf{m}})^2=\left(\frac{\hbar\omega}{\kappa\dot{\mathbf{m}}}\right)^2=\frac{\hbar\omega}{(2n+1)\kappa}. \tag{4.26}$$

Equation (4.23) now becomes

$$\begin{aligned}S_{\frac{\delta\Gamma}{\Gamma}}(f)&=\frac{\left(\frac{4\alpha}{3\pi f}\right)\hbar\omega}{(2n+1)\kappa(ec)^2}\\&=\frac{4\omega}{3\pi f(2n+1)\kappa c^3}\\&=\frac{2\hbar\omega^2}{3\pi fW\kappa c^3}.\end{aligned} \tag{4.27}$$

This quantum $1/f$ noise, proportional to the resonance frequency and inversely proportional to the number of quanta in the main oscillation mode, decreases when the energy in the main resonator mode increases. This is characteristic of quantum mechanical spontaneous emission noise in general. With $\omega=10^{10}$ rad/s and $W=0.01$ erg, we obtain about $10^{-27}/f\kappa$.

To estimate the coefficient κ, we write the mechanical energy, including both the equally contributing kinetic and elastic components, in the form

$$W=\frac{M_{\rm eff}v^2}{2} \tag{4.28}$$

where $M_{\rm eff}$ is a mass close to the mass M of the bar. Noting that the rate of change in the magnetic moment of the system, caused by the motion of the bar of length L with speed v, is

$$\begin{aligned}\dot{\mathbf{m}}&=\frac{\mathbf{n}SdI}{dt}+\frac{nIdS}{dt}=\frac{\mathbf{n}SBLv}{cL}\\&=\frac{\mathbf{n}SBLvc}{2\int\ln\left(\frac{R}{a_s}\right)ds}\end{aligned} \tag{4.29}$$

we find

$$\kappa=\frac{M_{\rm eff}v^2}{\dot{\mathbf{m}}^2}=M_{\rm eff}\left[\frac{cL}{SBL}\right]^2. \tag{4.30}$$

Here we introduced the area S and the inductance L of the ac circuit. We also introduced the approximate expression of L in terms of an integral around the whole circuit. It involves the radius as of the cross section of the electric wire used for the ac circuit, a_s a function of the length parameter s along the wire. We neglected the term with IdS/dt, because $S\omega\gg Lv$. We can approximate $S/2\int\ln(R/a_s)ds$ with $R/\langle\ln(R/a_s)\rangle$, where $R=S/l$ is the circuit area S divided by its length l. This way we obtain, e.g., $R'=S/2\int\ln(R/a_s)ds=300$ cm as an order of magnitude, and $c/R'=10^8$ Hz. With these notations and approximations, (4.30) becomes

$$\kappa=M_{\rm eff}\left[\frac{c}{R'BL}\right]^2. \tag{4.31}$$

With $M_eff=10^{-11}$ g, $L=10^{-3}$ cm, and $B=10^4$ Gauss, we obtain $\kappa=10^3\ {\rm cm}^{-1}$. Substituting into (4.6), we obtain

$$\begin{aligned}S_{\frac{\delta\Gamma}{\Gamma}}(f)&=\frac{\left(\frac{4\alpha}{3\pi f}\right)(R'BL)^2\hbar\omega}{(2n+1)M_{\rm eff}e^2c^4}\\&=\frac{4(R'BL)^2\omega}{3\pi f(2n+1)M_{\rm eff}c^5}\\&=\frac{2(R'BL)^2\hbar\omega^2}{3\pi fWM_{\rm eff}c^5}.\end{aligned} \tag{4.32}$$

For instance, with the above numerical example, with $\omega=10^{11}\ {\rm s}^{-1}$, and with $W=10^{-8}$ erg, we obtain $10^{-22}/f$.

Electrostatic Excitation of a Resonant Silicon Bar: The elementary act of dissipation is again the absorption of one phonon from the main resonator mode. This time, the quantum $1/f$ noise is caused by the sudden change in the rate of change of the dipole moment $\dot{\mathbf{p}}$ of the capacitor, when the phonon is absorbed. Replacing the current change $e\Delta\mathbf{v}$ this time with $\Delta\ \dot{\mathbf{p}}$, we obtain

$$S_{\frac{\delta\Gamma}{\Gamma}}(f)=\frac{4\alpha(\Delta\dot{\mathbf{p}})^2}{3\pi fe^2c^2}. \tag{4.33}$$

To calculate the change $\Delta\ \dot{\mathbf{p}}$, we note that $(\dot{\mathbf{p}})^2$ is proportional to the transversal vibration speed of the bar and to the total mechanical energy $W=(n+1/2)\hbar\omega$ in the main oscillation mode of the resonator,

$$\left(n+\frac{1}{2}\right)\hbar\omega=\frac{\kappa'(\dot{\mathbf{p}})^2}{2}. \tag{4.34}$$

Here κ' is a coefficient of proportionality easy to calculate. When a phonon is removed from the main MEMS resonator mode, the energy in (4.34) is reduced by the amount

$$\hbar\omega=\kappa'\dot{\mathbf{p}}\ \Delta\dot{\mathbf{p}}\,. \tag{4.35}$$

This yields

$$(\Delta\dot{\mathbf{p}})^2=\left(\frac{\hbar\omega}{\kappa'\dot{\mathbf{p}}}\right)^2=\frac{\hbar\omega}{(2n+1)\kappa'}. \tag{4.36}$$

Equation (4.32) now becomes

$$S_{\frac{\delta\Gamma}{\Gamma}}(f) = \frac{\left(\frac{4\alpha}{3\pi f}\right)\hbar\omega}{(2n+1)\kappa'(ec)^2} = \frac{4\omega}{3\pi f(2n+1)\kappa' c^3} = \frac{2\omega^2\hbar}{3\pi f W \kappa' c^3}. \tag{4.37}$$

This quantum $1/f$ noise, proportional to the resonance frequency and inversely proportional to the number of quanta in the main oscillation mode, decreases when the energy in the main resonator mode increases. This is characteristic of quantum mechanical emission noise in general. With $\langle\omega\rangle = 10^{12}$ rad/s and $W = 10^{-13}$ erg we obtain about $10^{-22}/f\kappa'$.

To estimate the coefficient κ', we write again the mechanical energy in the form

$$W = \frac{M_{\text{eff}} v^2}{2}. \tag{4.38}$$

Noting that the rate of change in the electric dipole moment of the system, caused by the motion of the bar of linear charge density q is

$$\dot{\mathbf{p}} = qLv \tag{4.39}$$

we find

$$\kappa' = \frac{M_{\text{eff}} v^2}{\dot{\mathbf{p}}^2} = \frac{M_{\text{eff}}}{q^2 L^2}. \tag{4.40}$$

With Meff $= 10^{-11}$ g, $L = 10^{-3}$ cm and $q = 0.6$ esu/cm, we obtain $\kappa = 2.7 \cdot 10^{-5}\ s^2\text{cm}^{-3}$. Substituting into (4.37), we obtain

$$S_{\frac{\delta\Gamma}{\Gamma}}(f) = \frac{\left(\frac{4\alpha}{3\pi f}\right) q^2 L^2 \hbar\omega}{(2n+1)M_{\text{eff}}(ec)^2} = \frac{4q^2L^2\omega}{3\pi f(2n+1)M_{\text{eff}} c^3} = \frac{2q^2L^2\hbar\omega^2}{3\pi f W M_{\text{eff}} c^3}. \tag{4.41}$$

For instance, with the above numerical example, with $\langle\omega\rangle = 10^{12}\ \text{s}^{-1}$, and with $W = 10^{-13}$ erg, we obtain $3 \cdot 10^{-18}/f$.

Finally, the quantum $1/f$ frequency fluctuations can be obtained from the formula

$$S_{\frac{\delta\omega}{\omega}} = \left(\frac{1}{4Q^4}\right) S_{\frac{\delta\Gamma}{\Gamma}} \tag{4.42}$$

which is derived below. This finally yields with (4.41)

$$S_{\frac{\delta\omega}{\omega}} = \frac{\left(\frac{1}{2Q^4}\right) q^2 L^2 \hbar\omega^2}{3\pi f W M_{\text{eff}} c^3}. \tag{4.43}$$

for the electrostatic capacitively coupled case, and, from (4.31)

$$S_{\frac{\delta\omega}{\omega}} = \frac{\left(\frac{1}{2Q^4}\right) (IL)^2 \hbar\omega^2}{3\pi f W M_{\text{eff}} c^5} \tag{4.44}$$

for the fractional frequency fluctuation spectrum exhibited by the magnetically driven MEMS resonator. The numerical estimated show that the electrostatically driven resonator is much noisier than the magnetically driven one when it comes to $1/f$ noise. This is because the magnetic dipole radiation is much weaker, being of higher order than the electric dipole radiation.

E. Classical Forms of Phase Noise

Phase noise is generated both classically and quantum mechanically. The quantum mechanical noise source is quantum $1/f$ noise, which is the main subject discussed here. However, there are also classical sources of noise, recently investigated by Vig [56] and caused by the factors described below.

Temperature Fluctuations: δT are particularly important in small resonators, such as MEMS resonators, due to the "bolometer effect." In thermal equilibrium, from thermodynamics

$$\left\langle(\delta T)^2\right\rangle = \frac{kT^2}{C} = \frac{kT^2}{c_v V} \tag{4.45}$$

where k is Boltzmann's constant and C the heat capacity of the resonating body, i.e., volumetric specific heat c_v, times volume V. Any temperature variations cause thermal dilatation and changes in the elastic constants and the speed of sound. These, in turn, affect the resonance frequency through the temperature coefficient $\alpha_T = d\nu/\nu dT x\nu$. For silicon MEMS resonators, Nguyen [65] reported $\alpha_T = -10^{-5}/K$. Denoting by G the thermal exchange rate, we obtain

$$\frac{Cd\delta T}{dt} = -G\delta T;$$
$$\delta T(t) = \delta T(0)\exp\left(-\frac{Gt}{C}\right);$$
$$\langle\delta T(t)\delta T(t+\tau)\rangle = \left\langle(\delta T)^2\right\rangle \exp\left(-\frac{Gt}{C}\right). \tag{4.46}$$

Therefore, using the Wiener–Khintchine theorem, the spectral densities of temperature fluctuations, of relative frequency fluctuations $y = \delta\nu/\nu$ and phase ϕ are

$$\left\langle (\delta T)^2 \right\rangle_f \equiv S_{\delta T}(f) = \frac{\left(\frac{4kT^2}{G}\right)}{\left[1 + \left(\frac{2\pi f C}{G}\right)^2\right]} \tag{4.47}$$

$$\left\langle \left(\frac{\delta\nu}{\nu}\right)^2 \right\rangle_f \equiv S_{\frac{\delta\nu}{\nu}}(f) = \frac{\left(\frac{4\alpha_T^2 kT^2}{G}\right)}{\left[1 + \left(\frac{2\pi f C}{G}\right)^2\right]} \tag{4.48}$$

$$\begin{aligned}\mathcal{L}(f) &= \left(\frac{\nu^2}{2f^2}\right) S_{\frac{\delta\nu}{\nu}}(f) \\ &= \frac{\left(\frac{\nu^2}{2f^2}\right)\left(\frac{4\alpha_T^2 kT^2}{G}\right)}{\left[1 + \left(\frac{2\pi f C}{G}\right)^2\right]}\end{aligned} \tag{4.49}$$

In the case of MEMS resonators with frequencies from 100 kHz to 10 GHz, these results have been graphed by J. Vig for heat exchange G caused by radiation, and by both radiation and conduction. Conduction turns out to be dominant in MEMS and NEMS with G between 1 and 5×10^{-6}, causing $\tau = C/G$ to be of the order of 10^{-5} s and smaller, so the second term in the denominator can be neglected. Thus

$$\begin{aligned}\mathcal{L}(f) &= \left(\frac{\nu^2}{2f^2}\right) S_{\frac{\delta\nu}{\nu}}(f) = \left(\frac{\nu^2}{2f^2}\right)\left(\frac{4\alpha_T^2 kT^2}{G}\right) \\ &\approx \left[-225 + 20\, lg\left(\frac{\nu}{f}\right)\right] \text{dBc}\end{aligned} \tag{4.50}$$

is a good approximation.

Note that the heat conduction rate G to the support heat sink is proportional to the thickness z and width W, while inversely proportional to the length L of the resonating MEMS bar. Therefore, for self-similar scaling of the size and volume, the frequency noise spectrum will be proportional with the $-1/3$ power of the volume V, and the proportionality with ν^2 may introduce an additional dependence of phase noise, roughly with $V^{-2/3}$ when the same resonant mode is used. In conclusion, an inverse proportionality of classical $1/f^2$ phase noise caused by temperature fluctuations on the resonant volume V can be expected as a first rough approximation

$$\mathcal{L}(f) = \left(\frac{\nu^2}{2f^2}\right) S_{\frac{\delta\nu}{\nu}}(f) = \left(\frac{\nu^2}{2f^2}\right)\left(\frac{4\alpha_T^2 kT^2}{G}\right) \approx \frac{\text{const}}{V}. \tag{4.51}$$

Johnson Noise, or Nyquist Noise: This is thermal noise in the motional resistance of the vibrating crystal, i.e., in the internal friction or dissipative mechanical resistance. It is caused by the scattering of phonons out of the main resonator mode into thermal modes, both scattering on thermal phonons and on crystal defects, including also impurities. It is the thermal equilibrium noise of the same resistance that also shows fundamental quantum $1/f$ noise as shown here. It is given by

$$\mathcal{L}(f) = \left(\frac{\nu^2}{2f^2}\right) S_{\frac{\delta\nu}{\nu}}(f) = \left(\frac{\nu^2}{2f^2}\right)\left(\frac{kT}{PQ_L^2}\right) \tag{4.52}$$

where Q_L is the loaded Q and P is the total power dissipated in the resonator plus load. Since the product $Q\nu$ is constant at about 10^6 Hz in MEMS resonators [56]

$$\begin{aligned}\mathcal{L}(f) &= \left(\frac{\nu^2}{2f^2}\right) S_{\frac{\delta\nu}{\nu}}(f) = \left(\frac{\nu^4}{2f^2}\right)\left(\frac{kT}{P\nu^2 Q_L^2}\right) \\ &\approx [40\, lg\nu - 20\, lgf - 400]\, \text{dB}\end{aligned} \tag{4.53}$$

for a drive level that produces a heating of 10 K of the resonator in steady state. For other drive levels, causing a heating of ΔT, $10\, lg(\Delta T/10)$ needs to be subtracted also

$$\begin{aligned}\mathcal{L}(f) &= \left(\frac{\nu^2}{2f^2}\right) S_{\frac{\delta\nu}{\nu}}(f) = \left(\frac{\nu^4}{2f^2}\right)\left(\frac{kT}{P\nu^2 Q_L^2}\right) \\ &\approx \left[40\, lg\nu - 20\, lgf - 10\, lg\left(\frac{\Delta T}{10}\right) - 400\right] \text{dB}.\end{aligned} \tag{4.54}$$

Here we have assumed that the heating is proportional with the drive level. The power dissipated in the resonator in stationary conditions scales with resonator volume like G, i.e., with $V^{-1/3}$, as shown in the preceding paragraph. Assuming, as is often done, that $Q_u \approx 3Q_l$, we may apply this to the total dissipated power P present in (4.54). The proportionality with ν^4 may introduce an additional dependence of phase noise, roughly with $V^{-4/3}$ when the same resonant mode is used. In conclusion, an inverse 5/3 power proportionality of classical $1/f^2$ phase noise caused by Johnson (or Nyquist) noise on the resonant volume V can be expected as a first rough approximation

$$\mathcal{L}(f) = \left(\frac{\nu^2}{2f^2}\right) S_{\frac{\delta\nu}{\nu}}(f) = \left(\frac{\nu^4}{2f^2}\right)\left(\frac{kT}{P\nu^2 Q_L^2}\right) \approx \frac{\text{const}^{\frac{5}{3}}}{V} \tag{4.55}$$

Comparing with the bolometer effect, Johnson noise will become important only at resonator frequencies above 10 MHz.

Acceleration Noise: Caused by random vibration, acceleration noise adds a phase noise contribution

$$\begin{aligned}\mathcal{L}(f) &= \left(\frac{\nu^2}{2f^2}\right) S_{\frac{\delta\nu}{\nu}}(f) = \Gamma^2 \langle a^2 \rangle_f \left(\frac{\nu^2}{2f^2}\right) \\ &= \Gamma^2 S_a(f) \left(\frac{\nu^2}{2f^2}\right)\end{aligned} \tag{4.56}$$

where Γ is the acceleration sensitivity of the resonance frequency and $\langle a^2 \rangle f = S_a(f)$ is the power spectral density of the acceleration caused by external vibration to which the MEMS resonator is subjected. The factor ν^2 introduces a $V^{-2/3}$ dependence of the phase noise spectrum in this case.

F. Total Phase Noise

By adding the classical phase noise contributions from the preceding section to a reasonable analytical form of the quantum $1/f$ phase noise result derived in Section III-G, we obtain the total phase noise $\mathcal{L}(f)$, with PSD of the frequency fluctuations shown inside the curly brackets and shown with a red curve at low v in Fig. 6

$$\mathcal{L}(f) = \left(\frac{\nu^2}{2f^2}\right)\left\{\frac{\left(\frac{\beta}{fQ^4}\right)}{\left[\frac{1}{V}+\frac{V}{\varepsilon^6}\right]} + \frac{\left(\frac{4\alpha_T^2 kT^2}{G}\right)}{\left[1+\left(\frac{2\pi fC}{G}\right)^2\right]^2} + \left(\frac{kT}{Q_l^2 P}\right) + \Gamma^2\left\langle(\delta a)^2\right\rangle_f\right\}. \quad (4.57)$$

The last three terms in the curly brackets are proportional to V^{-1}, $V^{-5/3}$, and $V^{-2/3}$, respectively, and yield the behavior sketched qualitatively in Fig. 6 with a red line on the left of the anthill shaped graph. The latter is predicted by the quantum $1/f$ theory for BAW and Si MEMS on the increasing branch of the anthill, and for SAW quartz, resonators on the decreasing branch. Note that the Q$1/f$ anthill curve increases when the modulation frequency is lowered, so the minimum on the red curve shifts to smaller volumes. That minimum is where the lowest phase noise of Si MEMS and quartz BAW resonators is obtained through optimization.

G. *Conclusions*

1) The quantum $1/f$ limit of BAW and SAW QCMs is given by simple formulas allowing calculation of the ultimate mass and concentration threshold of detection.
2) The devices are optimized by avoiding the $V = \varepsilon^3$ region.
3) The magnetic excitation sensors based on MEMS resonators have much lower $1/f$

V. Quantum $1/f$ Phase Noise in Oscillators

A. *Calculation of the FET and HFET—Based Amplifier Noise Figure F When the $1/f$ Noise Power Spectra $S_{\delta R/R}$ for the Channel and $S_{\delta RG/RG}$ for the Gate Are Known*

Summary: The connection between HFET channel resistance fluctuation noise and the noise figure F of the corresponding amplifier is derived here, in order to show how the various noise sources present in the channel and in the gate can be integrated.

The noise figure F of an amplifier stage is defined as shown in the equation at the bottom of the page. If, for instance, the amplifier stage (e.g., an FET or HFET) amplifies the thermal noise of a conductance gs connected between the input ports, with a current I_{Ch} present in the channel, the noise figure is as shown in (5.1), at the bottom of the next page. Here $S_{\delta R/R}$ and $S_{\delta RG/RG}$ are the (quantum $1/f$ and GR type) spectral densities of fractional resistance fluctuations in the channel resistance R_{Ch} and gate insulation conductance g_i, respectively, while $|Y_{\mathrm{tr}}|$ is the transadmittance, also known as transconductance (gm) at lower frequencies. This result derived below for F assumes that the noise source $S_{\delta RG/RG}$ in the gate insulation conductance g_i and the noise source $S_{\delta R/R}$ in the channel resistance R_{Ch} are uncorrelated. This is not always rigorously true, particularly at high frequencies, at which, however, the base-band $1/f$ noise is negligible; while phase noise matters. The phase noise is the one that persists with importance at high frequencies, more than amplitude noise, in most applications.

The minimal noise figure $F_{\min}$ is a good measure of the noise of the amplifier stage at intermediate values of g_s, R_{no} is a good noise measure for large values of g_s, and $g_{\mathrm{no}} = g_n + R_n g_i^2$ is a good noise measure for small values of g_s. From (1) and (5), $R_{\mathrm{no}} = R_n/(1-2R_n g_i) \approx R_n$ is the source resistance necessary to double the output power of the (short-circuited-input) amplifier stage. Also, $g_{\mathrm{no}}/(1-2R_n g_i) \approx g_{\mathrm{no}}$ is the source conductance needed in order to double the output of an amplifier, starting from $g_s = 0$. Note that R_n and g_n are defined by (5.8) and (5.9) below. *Finally, F turns out to be practically the same for common source, common gate, and common drain circuits.* The $\approx$ sign assumes $g_i \ll 1/2R_n$, i.e., that there is good gate insulation. The minimal noise figure

$$\begin{aligned} F_{\min} &= 1 + 2R_n\left\{g_i + \left(\frac{g_n}{R_n} + g_i^2\right)^{\frac{1}{2}}\right\} \\ &= 1 + 2\left\{\frac{\left[\frac{4kT_o}{R_{\mathrm{Ch}}} + I_{\mathrm{Ch}}^2 S_{\frac{\delta R}{R}}\right]}{4kT_o|Y_{\mathrm{tr}}|^2}\right\} \\ &\quad \times \left\{g_i + \left[\frac{|Y_{\mathrm{tr}}|^2\left(4kT_o g_i + I_G^2 S_{\frac{\delta R_G}{R_G}}\right)}{\left(\frac{4kT_o}{R_{\mathrm{Ch}}} + I_{\mathrm{Ch}}^2 S_{\frac{\delta R}{R}}\right)} + g_i^2\right]^{\frac{1}{2}}\right\} \end{aligned}$$

$$F = \frac{\left[\text{Output noise power } \langle\Delta V^2\rangle_f\right]}{\left[\text{Output noise power of the noiseless amplifier or device}\right]}.$$

$$\begin{aligned} F &= \{4kT_o g_s + (4kT_o g_i + I_G{}^2 S_{\delta RG/RG}) + (g_s+g_i)^2\left[(4kT_o/R_{\mathrm{Ch}} + I_{\mathrm{Ch}}{}^2 S_{\delta R/R})/|Y_{\mathrm{tr}}|^2\right]\}/ \\ 4kT_o g_s &= 1 + \left[g_i + I_G{}^2 S_{\delta RG/RG}/4kT_o\right]/g_s + (g_s+gi)^2\{\left[4kT_o/R_{\mathrm{Ch}} + I_{\mathrm{Ch}}^2 S_{\delta R/R}/|Y_{\mathrm{tr}}|^2\right]\}/4kT_o g_s. \quad (5.1) \end{aligned}$$

$$(5.2)$$

is obtained for

$$\begin{aligned} g_s = g_{\mathrm{sOPT}} &= \left(g_i^2 + \frac{g_n}{R_n}\right)^{\frac{1}{2}} \\ &= \left\{ g_i^2 + \frac{|Y_{\mathrm{tr}}|^2\left(4kT_o g_i + I_G^2 S_{\frac{\delta R_G}{R_G}}\right)}{\left(\frac{4kT_o}{R_{\mathrm{Ch}}} + I_{\mathrm{Ch}}^2 S_{\frac{\delta R}{R}}\right)} \right\}^{\frac{1}{2}}. \end{aligned} \quad (5.3)$$

Note that the present results assume a negligible direct input–output coupling (and therefore uncorrelated fluctuations in the gate and channel resistances), as can be obtained at low frequencies, and for low-frequency noise processes leading to generation of phase noise close to the carrier at high and ultrahigh frequencies. It is easy to relax this neglect of correlation.

Derivation: In general, to calculate the noise figure of an amplifier stage, one:

1) draws the equivalent circuit;
2) includes all noise sources:
   a) $i_i = (4kT_o g_n \Delta f)^{1/2}$, representing $1/f$, GR, and thermal rms noise current of the gate in terms of the equivalent noise conductance g_n of the gate insulation conductance g_i;
   b) $e_n = (4kT_o R_n \Delta f)^{1/2}$, representing $1/f$, GR, and thermal rms input-referred voltage noise of the channel in terms of the equivalent input-referred noise resistance R_n of the channel;
3) calculates the mean square value $\langle i_{\mathrm{out}}^2\rangle = \langle v_g^2\rangle |Y_{\mathrm{tr}}|^2$ of the output noise; and

$$\left\langle i_{\mathrm{out}}^2\right\rangle = \left[\frac{4kT_o(g_s+g_n)\Delta f}{(g_s+g_i)^2} + 4kT_o R_n \Delta f\right]|Y_{\mathrm{tr}}|^2 \quad (5.4)$$

4) defines

$$\begin{aligned} F &= \left[\frac{\left\langle i_o^2\right\rangle}{(\text{contribution of the noise source to } \langle i_o^2\rangle)}\right] \\ &= \frac{\left\langle i_o^2\right\rangle}{\left[\frac{4kT_o g_s \Delta f |Y_{\mathrm{tr}}|^2}{(g_s+g_i)^2}\right]}: \\ F-1 &= \frac{g_n}{g_s} + \frac{(g_s+g_i)^2 R_n}{g_s} \\ &= 2R_n g_i + R_n g_s + \frac{\left(g_n + g_i^2 R_n\right)}{g_s}. \end{aligned} \quad (5.5)$$

This function of g_s has a minimal value

$$F_{\min} - 1 = 2R_n g_i + 2\left(R_n g_n + g_i^2 R_n^2\right)^{\frac{1}{2}} \quad (5.6)$$

at

$$g_s = g_{\mathrm{sOPT}} = \left(g_i^2 + \frac{g_n}{R_n}\right)^{\frac{1}{2}}. \quad (5.7)$$

For FETs and HFETs we write

$$4kT_o g_n(f) = 4kT_o g_i + I_G^2 S_{\frac{\delta R_G}{R_G}} \quad (5.8)$$

and

$$4kT_o R_n = \frac{\left[\frac{4kT_o}{R_{\mathrm{Ch}}} + I_{\mathrm{Ch}}^2 S_{\frac{\delta R}{R}}\right]}{|Y_{\mathrm{tr}}|^2}. \quad (5.9)$$

Therefore

$$F-1 = \frac{\left[g_i + \frac{I_G^2 S_{\frac{\delta R_G}{R_G}}}{4kT_o}\right]}{g_s} + (g_s+g_i)^2 \frac{\left[\frac{4kT_o}{R_{\mathrm{Ch}}} + I_{\mathrm{Ch}}^2 S_{\frac{\delta R}{R}}\right]}{4kT_o g_s |Y_{\mathrm{tr}}|^2} \quad (5.10)$$

and

$$\begin{aligned} F_{\min} - 1 &= 2R_n\left\{g_i + \left(\frac{g_n}{R_n} + g_i^2\right)^{\frac{1}{2}}\right\} \\ &= 2\left\{\frac{\left[\frac{4kT_o}{R_{\mathrm{Ch}}} + I_{\mathrm{Ch}}^2 S_{\frac{\delta R}{R}}\right]}{4kT_o|Y_{\mathrm{tr}}|^2}\right\} \\ &\quad \times \left\{ g_i + \left[\frac{|Y_{\mathrm{tr}}|^2\left(4kT_o g_i + I_G^2 S_{\frac{\delta R_G}{R_G}}\right)}{\left(\frac{4kT_o}{R_{\mathrm{Ch}}} + I_{\mathrm{Ch}}^2 S_{\frac{\delta R}{R}}\right)} + g_i^2\right]^{\frac{1}{2}} \right\} \end{aligned} \quad (5.11)$$

for

$$\begin{aligned} g_s = g_{\mathrm{sOPT}} &= \left(g_i^2 + \frac{g_n}{R_n}\right)^{\frac{1}{2}} \\ &= \left\{ g_i^2 + \frac{|Y_{\mathrm{tr}}|^2\left(4kT_o g_i + I_G^2 S_{\frac{\delta R_G}{R_G}}\right)}{\left(\frac{4kT_o}{R_{\mathrm{Ch}}} + I_{\mathrm{Ch}}^2 S_{\frac{\delta R}{R}}\right)} \right\}^{\frac{1}{2}}. \end{aligned} \quad (5.12)$$

Here $S_{\delta R/R}$ and $S_{\delta RG/RG}$ are the quantum $1/f$ and GR-type spectral densities of fractional resistance fluctuations in the channel and gate insulation, respectively, while $|Y_{\mathrm{tr}}|$ is the transadmittance, also known as transconductance at lower frequencies.

Considering the input conductance g_i to be negligible, and neglecting also the gate noise $S_{\delta RG/RG}$, as was reasonable to do for our FETs at the low gate voltages measured, we obtain

$$F - 1 \approx \frac{\left[\frac{4kT_o}{R_{\mathrm{Ch}}} + I_{\mathrm{Ch}}^2 S_{\frac{\delta R}{R}}\right]}{4kT_o R_s |Y_{\mathrm{tr}}|^2}. \quad (5.13)$$

If, on the other hand, we neglect only the current noise of the gate current, we get

$$F-1=\frac{g_i}{g_s}+\frac{(g_s+g_i)^2\left[\frac{4kT_o}{R_{\mathrm{Ch}}}+I_{\mathrm{Ch}}^2 S_{\frac{\delta R}{R}}\right]}{4kT_o g_s |Y_{\mathrm{tr}}|^2} \tag{5.14}$$

and

$$\begin{aligned} F_{\min}-1 &= 2R_n\left\{g_i+\left(\frac{g_i}{R_n}+g_i^2\right)^{\frac{1}{2}}\right\} \\ &= 2\left\{\frac{\left[\frac{4kT_o}{R_{\mathrm{Ch}}}+I_{\mathrm{Ch}}^2 S_{\frac{\delta R}{R}}\right]}{4kT_o|Y_{\mathrm{tr}}|^2}\right\} \\ &\quad\times\left\{g_i+\left[\frac{|Y_{\mathrm{tr}}|^2 4kT_o g_i}{\left(\frac{4kT_o}{R_{\mathrm{Ch}}}+I_{\mathrm{Ch}}^2 S_{\frac{\delta R}{R}}\right)+g_i^2}\right]^{\frac{1}{2}}\right\} \end{aligned} \tag{5.15}$$

for

$$\begin{aligned} g_s = g_{s\mathrm{OPT}} &= \left(g_i^2+\frac{g_i}{R_n}\right)^{\frac{1}{2}} \\ &= \left\{g_i^2+\frac{|Y_{\mathrm{tr}}|^2 4kT_o g_i}{\left(\frac{4kT_o}{R_{\mathrm{Ch}}}+I_{\mathrm{Ch}}^2 S_{\frac{\delta R}{R}}\right)}\right\}^{\frac{1}{2}}. \end{aligned} \tag{5.16}$$

Our measurements performed in St. Louis on the UCSB HFETs of Mishra *et al.* on three substrates (Table 2) give both R_{Ch} and $S_{\delta R/R}$ as a function of I_{Ch} and V_G, while the transconductance $g_m \approx |Y_{\mathrm{tr}}|$ is known from the I–V characteristics. Therefore, we can easily determine a noise figure from each of our measurements with this simple last formula for each V_G, drain bias V_{DS}, or channel current I_{Ch}, and for any given source resistance R_s and $|Y_{\mathrm{tr}}|$ While the noise figure depends on the source resistance and on the bias I_{Ch}, our results are of intrinsic nature, independent of these circumstances, allow the determination of the effective Hooge constant, allow easy comparisons with the quantum $1/f$ theory, and also allow us to find the noise figure (and, knowing the gate conductance g_i, also $F_{\min}$) easily for any application involving the given HFET.

B. *Quantum $1/f$ Noise Sources in GaN HFETs*

Gate Noise: The gate leakage current results in relatively large noise and can contribute considerably to phase noise. This large contribution is caused by the piezoelectric quantum $1/f$ effect affecting currents present in sufficiently large samples of spontaneously polarized ferroelectric material, with a 10^6 times larger quantum $1/f$ noise coefficient introduced by the speed of sound replacing the speed of light in Sommerfeld's fine structure constant. It is enhanced also because gate potential fluctuations appear amplified in the channel current. Our theory yields a power spectrum of gate resistance fluctuations

$$\mathbf{S}_{\frac{\delta \mathbf{RG}}{\mathbf{RG}}}=\frac{\boldsymbol{\alpha}_{\mathbf{G}}}{\mathbf{N_G f}};\quad \boldsymbol{\alpha}_{\mathbf{G}}\approx 0.2=\text{piezo }\frac{Q1}{f}\text{ coefficient.} \tag{5.17}$$

Here $\mathbf{N_G} = I_G\tau$ where I_G is the gate current and τ is the life time of the carriers in the AlGaN gate insulation.

To understand the large value of α, we mention that the piezoelectric Q$1/f$ coefficient, like the electrodynamic one, is also found [75], [76] by combining the conventional and coherent parts in a weighted sum

$$\begin{aligned} \boldsymbol{\alpha}_H = \mathrm{fNS}_{\frac{\delta j}{j}}(f) &= \left[\frac{1}{(1+s')}\right]\left(\frac{4g}{3\pi}\right)\left(\frac{\boldsymbol{\Delta}\mathbf{k}}{k_s}\right)^2 \\ &\quad+\left[\frac{s'}{(1+s')}\right]\left\{\frac{2g}{\pi\left[1-\left(\frac{\langle\mathbf{k}\rangle}{k_s}\right)^2\right]}\right\} \end{aligned} \tag{5.18}$$

where v_s is the speed of sound, $\langle\mathbf{k}\rangle = m^*\langle\mathbf{v}\rangle/\hbar$, $|\langle\mathbf{v}\rangle| = u$ is the drift velocity of the carriers, $\boldsymbol{\Delta}\mathbf{k}/k_s = \boldsymbol{\Delta}\mathbf{v}/v_s$, and [75], [76]

$$k_s=\frac{m^* v_s}{\hbar};\quad s'=\left(\frac{gN'\hbar}{\pi m^* v_s}\right)\left(\frac{v_s}{u}\right)^3 F\left(\frac{u}{v_s}\right). \tag{5.19}$$

Here N' is the number of carriers per unit length of the sample in the direction of current flow, and

$$\begin{aligned} F\left(\frac{u}{v_s}\right) &= 2\left(\frac{u}{v_s}\right)\left\{1+\frac{1}{\left[1-\left(\frac{u}{v_s}\right)^2\right]}\right\} \\ &\quad+\ln\left[1-\left(\frac{u}{v_s}\right)\right]^2-\ln\left[1+\left(\frac{u}{v_s}\right)\right]^2. \end{aligned} \tag{5.20}$$

For $u/v_s \ll 1$,

$$\begin{aligned} F\left(\frac{u}{v_s}\right) &= \left(\frac{2}{3}\right)\left(\frac{u}{v_s}\right)^3. \quad \text{Then } s'=\left(\frac{2gN'\hbar}{3\pi m^* v_s}\right) \\ &\approx N'.10^{-7}\ \text{cm}. \end{aligned} \tag{5.21}$$

For $1-(u/v_s) \ll 1$

$$F\left(\frac{u}{v_s}\right)=\frac{1}{\left[1-\left(\frac{u}{v_s}\right)\right]}. \tag{5.22}$$

Due to the small number of carriers, their drift velocity is close to the sound velocity in the AlGaN gate, and the condition $1-(u/v_s) \ll 1$ is satisfied. Then we obtain

$$s'=\left(\frac{gN'\hbar}{\pi m^* v_s}\right)\left(\frac{v_s}{u}\right)^2\left\{\frac{1}{\left[1-\left(\frac{u}{v_s}\right)\right]}\right\} \tag{5.23}$$

which can be larger than one. In conclusion, due to the large value of s', the first term in (5.18) is negligible, and the coefficient $s'/(1+s')$ of the second term is one. From the graph in Kee [71, Fig. 4.1, p. 48], we find that g is about three; therefore, $a \approx 0.2$, as mentioned above, for AlGaN, which is stiffer.

Channel Noise: The noise present in the GaN/AlGaN HFET's channel was derived and discussed in Section III above. Including also the source and drain resistances, in

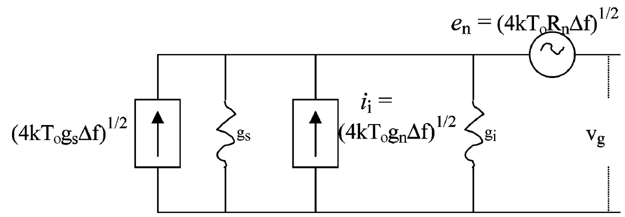

Fig. 7. Equivalent circuit of an HFET amplifier with noise sources referred to the input.

terms of the HFET's channel resistance R_{Ch} and of the current I_{Ch} through it, we obtain

$$\begin{aligned} S_R &= S_{\mathrm{RS}} + S_{\mathrm{RD}} + S_{\mathrm{Rch}} + \frac{4kTR_{\mathrm{ch}}}{I_{\mathrm{ch}}^2} \\ &= \frac{4kTR_{\mathrm{ch}}}{I_{\mathrm{ch}}^2} + \frac{R_S^3 e\mu_S\alpha_S}{fL_S^2} + \frac{R_D^3 e\mu_D\alpha_D}{fL_D^2} \\ &\quad + \frac{1}{\mu f I_{\mathrm{Ch}}}\left[\frac{\alpha_H^{\mathrm{coh}}}{qZ^2D_{\mathrm{eff}}^2V_{\mathrm{th}}} + \frac{\alpha_H^{\mathrm{conv}}qv_s^2R_{\mathrm{Ch}}}{I_{\mathrm{ch}}}\xi\Theta(\xi)\right] \\ \xi &\equiv 1 - \frac{V_G^*}{R_{\mathrm{Ch}}I_{\mathrm{Ch}}} + \frac{V_{\mathrm{th}}}{R_{\mathrm{Ch}}I_{\mathrm{Ch}}}; \\ \Theta(\xi) &\equiv \frac{(1+sign\xi)}{2} \end{aligned} \tag{5.24}$$

Here the source, channel, and drain resistances form the total resistance: $R_S + R_{\mathrm{Ch}} + R_D = 1/G_m$; where G_m is the total HFET conductance.

C. Oscillator Phase Noise

The oscillator can be modeled in a first approximation as an oscillant circuit (Fig. 7) described by a harmonic oscillator equation

$$\frac{d^2x}{dt^2} + \frac{2\gamma dx}{dt} + \omega_0^2 x = F_0\exp(i\omega t). \tag{5.25}$$

In Fig. 7, $-G_m(V_o)$ is a negative conductance that represents the active element, the force $F_0\exp(i\omega t)$, causing the oscillations. This force, or emf, is assumed to be free of fluctuations. The fluctuations are present in the dissipative element that may be present in the active device and in the resonator. The solution for x, which can be the current or the voltage in the oscillant circuit, is

$$\begin{aligned} (x, I, V) &= (x_0, I_0, V_0)\exp(i\omega t); \\ |x_0|^2 &= \frac{|F_0|^2}{\left[(\omega_0^2 - \omega^2)^2 + 4\gamma 2\omega^2\right]} \end{aligned} \tag{5.26}$$

The resonance condition

$$\frac{d|x_0|^2}{d\omega} = 0$$

yields

$$\omega_r^2 = \omega_o^2 - 2\gamma^2. \tag{5.27}$$

Conventional quantum $1/f$ noise is a fundamental quantum fluctuation present in quantum mechanical cross sections and process rates. The latter determine the dissipation in quartz crystals and in general in resonant systems of any kind. Considering, therefore, fluctuations of the dissipative constant γ, we obtain for the resulting frequency fluctuations of the arbitrary resonant system

$$\omega_r\delta\omega_r = -2\gamma\delta\gamma; \quad \frac{\delta\omega_r}{\omega_r} = -2\left(\frac{\gamma}{\omega_r}\right)^2\frac{\delta\gamma}{\gamma}. \tag{5.28}$$

With $y \equiv \delta\omega_r/\omega_r$ and with $2\gamma/\omega$ being the quality factor Q, we obtain the frequency fluctuations power spectrum

$$S_y(f) = 4\left(\frac{\gamma}{\omega_r}\right)^4 S_{\frac{\delta\gamma}{\gamma}} = \left(\frac{1}{4Q^4}\right)S_{\frac{\delta\gamma}{\gamma}}. \tag{5.29}$$

This defines the phase noise that is to be expected in first approximation. However, there are also contributions from the source and drain series resistances, and from the gate leakage current. Together with the channel noise shown in (5.24), they define the total quantum $1/f$ frequency fluctuation noise $S_y^{Q1/f}$ and the corresponding phase noise $\mathcal{L}(f)$.

D. Total $1/f$-Type Phase Noise S_y^H

In terms of R, R_G, I_{Ch}, and I_G, with $R_S + R_{\mathrm{Ch}} + R_D = R$, our goal is to find the total quantum $1/f$ frequency fluctuation noise $S_y^H = \mathrm{Const}/f = S_{\delta\omega/\omega}$, including also all thermal noise sources at the end. The quantum $1/f$ resistance fluctuations in the channel, source, drain, and gate are independent, because they are fluctuations of different scattering cross sections and process rates. According to (5.11), (3.13), and (3.14), we obtain, by including the fluctuations of the channel resistance induced by the gate resistance fluctuations

$$\begin{aligned} S_R = &S_{\mathrm{RS}} + S_{\mathrm{RD}} + S_{\mathrm{Rch}} \\ &+ \frac{4kT(g_n+g_s)}{(g_i+g_s)^2I_{\mathrm{Ch}}^2)|R_{\mathrm{Ch}}Y_{\mathrm{tr}}|^2} \end{aligned} \tag{5.30}$$

$$\begin{aligned} = &\frac{R_S^3e\mu_S\alpha_S}{fL_S} + \frac{R_D^3e\mu_D\alpha_D}{fL_D} + \frac{4kTR_{\mathrm{ch}}}{I_{\mathrm{ch}}^2} + \frac{1}{\mu f I_{\mathrm{Ch}}} \\ &\times\left[\frac{\alpha_H^{\mathrm{coh}}}{qZ^2D_{\mathrm{eff}}^2V_{\mathrm{th}}} + \frac{\alpha_H^{\mathrm{conv}}qv_s^2R_{\mathrm{Ch}}}{I_{\mathrm{ch}}}\xi\Theta(\xi)\right] \\ &+ \frac{4kT(g_n+g_s)}{(g_i+g_s)^2I_{\mathrm{Ch}}^2)|R_{\mathrm{Ch}}Y_{\mathrm{tr}}|^2}. \end{aligned} \tag{5.31}$$

Here we included the noise conductance of the gate $g_n = g_i + I_G^2S_{\delta RG/RG}/4kT$, according to (5.8)–(5.11), with $y \equiv \omega/\omega$. We are now writing the corresponding phase noise. The following equations provide the quantum $1/f$ frequency fluctuations component, which is dominant close to the carrier, arising from the GaN/AlGaN HFETs. They also provide the frequency fluctuation from thermal noise in the gate and the channel.

To this result we have to add the well-known contribution of the sidebands arising from device nonlinearity (NSB part)

$$
\begin{aligned}
S_y^H = \frac{R_{\mathrm{Ch}}^{-2}}{4Q^4} \Bigg\{ & \frac{1}{\mu f I_{\mathrm{Ch}}} \left[\frac{\alpha_H^{\mathrm{coh}}}{qZ^2 D_{\mathrm{eff}}^2 V_{\mathrm{th}}} + \frac{\alpha_H^{\mathrm{conv}} q v_s^2 R_{\mathrm{Ch}}}{I_{\mathrm{Ch}}} \xi \Theta(\xi) \right] \\
& + \frac{\alpha_s}{f N_s} R_s^2 + \frac{\alpha_D}{f N_D} R_D^2 \\
& + \frac{4kT_o (g_s + g_n)}{(g_s + g_i)^2 I_{\mathrm{Ch}}^2} |R_{\mathrm{Ch}} Y_{tr}|^2 + \frac{4kTR_{\mathrm{Ch}}}{I_{\mathrm{Ch}}^2} \Bigg\}; \\
\xi \equiv 1 - & \frac{V_G^*}{R_{\mathrm{Ch}} I_{\mathrm{Ch}}} + \frac{V_{\mathrm{th}}}{R_{\mathrm{Ch}} I_{\mathrm{Ch}}}; \\
\Theta(\xi) \equiv & \frac{(1 + sign \xi)}{2}.
\end{aligned} \tag{5.32}
$$

This part can be reduced by operating the HFET at saturation, and restricting the dynamical range. Furthermore, partial compensation measures [see (5.32)] are possible for this classical part, as shown, e.g., by A. Hajimiri (HJM) [5]. Therefore,

$$S_y = S_y^{Q\frac{1}{f}} + S_y^{\mathrm{HJM}} + S_y^{\mathrm{NSB}}. \tag{5.33}$$

The phase noise at a frequency $\Delta\nu = f$ from the carrier frequency is given most often not in terms of frequency fluctuations, but in dBc, i.e.,

$$\mathcal{L}(f) = \mathcal{L}(\Delta\nu) = 10 \log \left[\left(\frac{1}{2}\right) \left(\frac{\omega}{2\pi f}\right)^2 S_y(f) \right]. \tag{5.34}$$

This all can now be applied to a practical example of GaN/AlGaN HFET-based oscillator.

E. Example: R. York—H. Xu—BST-Capacitor-Based Oscillator With AlGaN/GaN HFET

Consider now as a practical example the oscillator of R. York and H. Xu at UCSB (Fig. 8), developed as part of our Ultralow Phase Noise MURI Program. It uses a $\mathrm{BaSr(TiO_3)_2}$ bypass capacitor, as seen in Fig. 9. Its frequency is $\nu_o = 5$ GHz; its unloaded quality factor is $Q_u \approx 23$, and the loaded quality factor is estimated to be about $Q_l = 10$. From Table 2, we find for the HFET channel that provides the dissipation in the oscillator, approximately

$$\frac{S_R}{R}^2 \approx \frac{10^{-10}}{f}. \tag{5.35}$$

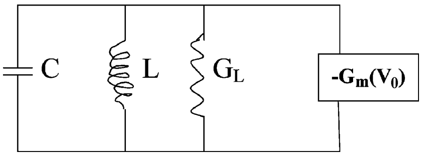

Fig. 8. Equivalent circuit of an oscillator, with active element shown as a negative conductance.

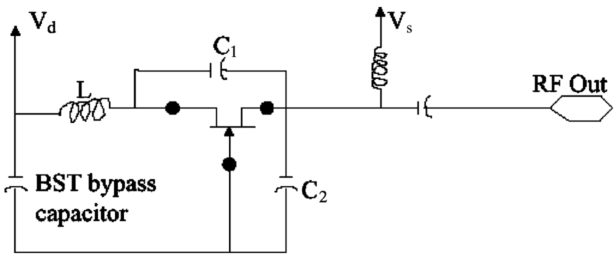

Fig. 9. GaN/AlGaN HFET-based oscillator of R. York and X. Hu (UCSB).

Considering also negligible gate noise, $4kTg_n \approx 0$, we obtain, from Q$1/f$ theory

$$S_y = \frac{\left(\frac{S_R}{R^2}\right)}{4Q_l^4 f} = \frac{10^{-10}}{4 \cdot 10^4 f} = \frac{2.5 \cdot 10^{-15}}{f} \tag{5.36}$$

and in phase noise language

$$
\begin{aligned}
\mathcal{L}(f) = L(\Delta\nu) &= 10 \log \left[\left(\frac{1}{2}\right) \left(\frac{\omega}{2\pi f}\right)^2 S_y(f) \right] \\
&= -45 \text{ dBc@1 kHz}
\end{aligned} \tag{5.37}
$$

or about -105 dBc@100 kHz.

Note that experimentally, $\mathcal{L}(100 \text{ KHz}) = -105$ dBc was measured, in excellent agreement with our rough estimate.

It is interesting to note that for $Q = 10^4$

$$\mathcal{L}(f) = -165 \text{ dBc@1 kHz}.$$

Therefore, it would be advisable to use special high-frequency MEMS resonators.

VI. Discussion

The research presented in this paper has considerable relevance for many military and civilian industrial applications. It is based on a simple derivation of the conventional and coherent quantum $1/f$ effects in Section II, resulting in a formula combining both effects as displayed in Fig. 1. This shows that the present miniaturization stage of electronic devices is affected by increased conventional quantum $1/f$ noise on the left side of the graph. The period in the 1980s and 1990s when devices where scaled down with impunity is over. Indeed, the transition from the larger coherent to the smaller conventional quantum $1/f$ effect (Q$1/f$E) is behind us, being represented by the horizontal part of the α/N graph. Therefore, there is increased need for quantum $1/f$ optimization of device, to reduce $1/f$ noise and phase noise, increasing the stability of the system.

The practical importance of phase noise is tremendous. A 10-dB reduction in the noise floor will reduce the bit-error rate by a factor of 10^{-6} in DSP systems that process real-time inputs in a battlefield environment. In a Doppler radar, from the R^{-4} law, a 24-dB reduction in the noise floor corresponds to a fourfold increase in range R. A new generation of low-noise electronic devices, improving both high-power systems (radars, radio, TV, microwave and THz transmitters, etc.) and ultralow power minireceivers, MEMS sensors, MEMS frequency standards, THz receivers, etc., is becoming possible due to advances in material processing and due to our better handle on $1/f$ noise and on the resulting phase noise (Section IV). This poorly understood subject was described with the help of the so-called Leeson formula. The present paper introduces a modification of this basic engineering formula with an additional Q^{-4} quantum 1/f term that is dominant for high-tech, high-stability oscillators, in any frequency domain. This fundamental breakthrough is of tremendous practical importance for the modern high-tech industry. It will be reflected in the quality of future military and civilian devices and systems across the board.

The quantum $1/f$ formula was used to provide for the first time a scientific calculation and a practical engineering formula for $1/f$ noise in GaN/AlGaN HFETs. The agreement with the experimental data of Balandin [31], Wang [32], and Viswanathan *et al.* [35] from the University of California, Riverside, is very good. The same good agreement is found with measurements performed by us in the St. Louis quantum $1/f$ lab on GaN/AlGaN HFETs provided by U. Mishra's group from UCSB. HFETs are of importance for military and civilian applications, being essential for low phase noise in the new generation of solid-state high-power RF and microwave generators.

RTDs have a negative differential resistance region in their current voltage characteristic. RTDs (Section III) are ideal for microwave generation almost up to the THz region. The quantum $1/f$ theory was applied by the author to find both the $1/f$ noise of the RTD and the resulting phase noise of the oscillator (generator with resonator) based on it. This allows for the first time for a scientific optimization of materials, devices, and systems for this application.

Of major importance is the early detection of an attack with biological or chemical weapons, in particular an attack with anthrax, smallpox, the plague, poliomyelitis, nerve gas, etc. This research, giving for the first time the quantum limits of, and optimization tools for, the resonant (and also nonresonant, as can be shown), biological and chemical sensors (Section III) was extended to MEMS at the suggestion of Dr. J. Vig (US Army CECOM). In general, the quantum $1/f$ theory and engineering formulas developed here allow for the optimization of both design and implementation of novel, completely monolithic integrated MEMS resonators and sensors. The quantum $1/f$ formula obtained for MEMS shows that when its is smaller than the coherence length of phonons, which is usually the case, a reduction in volume will reduce phase noise in proportion to $1/V$, up to a point where the classical bolometer effect's temperature fluctuations become dominant. There is an optimal size determined by the quantum $1/f$ formula, visible on Handel's anthill curve. In other resonators, larger than the coherence length, the stability increases proportional with the volume V.

The FET-based sensors and other sensors included in the electronic nose have also been perfected now to the point where they have reached their quantum limit. They are therefore limited by the quantum $1/f$ effect, and subject to Q$1/f$ optimization. There also was successful work presented in this paper on quantum $1/f$ effect in spin-polarized transport including nanodevices.

In conclusion, the present investigation is relevant in many ways for science and technology. It is important for the following military and civilian solid state and high-frequency research efforts.

1) Nanoscale science and technologies: They all face a mountain of $1/f$ noise and phase noise, according to left part on the lower curve on Fig. 1, Section II. The left part is the part relevant for the conventional quantum $1/f$ effect affecting the small device dimensions encountered in the nanometric domain. The transition region from coherent to conventional Q$1/f$E was applicable to dimensions in the micrometric domain, and corresponded to the horizontal part of the lower graph in Fig. 1. It was responsible for a lower noise penalty in the last two decades of device downscaling.
2) Terahertz and ultrafast electronics: The phase noise close to the carrier is determined by the quantum $1/f$ effect in all generators and detectors, as exemplified on RTDs in Section III above.
3) Advanced device concepts: The authors' simple quantum $1/f$ formulas are universally applicable. They allow for the analytical or/and numerical optimization of any high-tech device or system, and for the design of novel devices, based on chosen figures of merit and precise analytical expressions knowledge of how the quantum $1/f$ effect affects their performance.
4) Mixed technologies—electronics, photonics, acoustics, and magnetics: Here the quantum $1/f$ noise affects the transducers, the sensors linking these components, and each of the components individually. Optimization proceeds in three stages, materials, devices, and systems. Each electronic and electron–phonon scattering process, each piezo-phononic process, every spin-flip—they are all affected in their rate by quantum $1/f$ fluctuations, as we have seen, described by simple fundamental formulas given in this paper, with no free or adjustable parameters.
5) Ultralow-power technology: By reducing the noise in the quantum $1/f$ noise optimization process, one can reduce the logical swings that are needed in circuits, and therefore one can save power. The reduction of phase noise increases selectivity and reduces both the need for very powerful transmitters, and for very large ampli-

fication coefficients, therefore enabling ultralow-power technologies.

From our present vantage point, we may conclude that the quantum $1/f$ effect is inherently important in most high-technology applications. Indeed, the latter are based on total control of a physical or biological system by humans, in which all known classical instabilities and noise sources have been eliminated, or are under control. In this situation, when nothing else should keep fluctuating, the fundamental quantum $1/f$ fluctuations of physical cross sections, process rates, and currents, introduced in Section II above, invariably come to the forefront, destabilizing the system and setting the limits of achievable performance. Understanding of this basic fact and new aspect of quantum mechanics will generate a revolution in science and technology, based on a new generation of optimized, more stable, economical, and sensitive hardware, instrumentation, and standards.

ACKNOWLEDGMENT

Important contributions to this paper by Christian A. Fazi and Frank J. Crowne, who both collaborated in this work, are acknowledged with gratitude. The authors would like to thank D. Woolard, J. Vig, U. Mishra, R. York, H. Dietrich, J. Zolper, G. Witt, L. Cooper, and L. Chen for many useful discussions, samples/devices from UCSB, and suggestions. Support from ARO, the Ultra-Low Phase Noise MURI, ONR, and AFOSR is thankfully acknowledged, as well as earlier NSF and NEDO of Japan support.

REFERENCES

[1] A. van der Ziel, *Noise in Solid State Devices and Circuits*. New York: Wiley, 1986, ch. 11.

[2] P. H. Handel, "Nature of $1/f$ phase noise," *Phys. Rev. Lett.,* vol. 34, pp. 1495–1498, 1975.

[3] ——, "Nature of $1/f$ frequency fluctuations in quartz crystal resonators," *Solid State Electron.,* vol. 22, pp. 875–876, 1979.

[4] R. G. Rodgers, *Low Phase Noise Microwave Oscillator Design*. Boston, MA: Artech House, 1991.

[5] A. Hajimiri, *The Design of Low Noise Oscillators*. Boston, MA: Kluwer, 1999.

[6] J. B. Johnson, "The Schottky-effect in low-frequency circuits," *Phys. Rev.,* vol. 26, pp. 71–85, 1925.

[7] A. L. Mcwhorter, "$1/f$ noise and related surface effects in germanium," MIT Lincoln Lab. Rep., Lexington, MA, 1955, p. 80.

[8] P. H. Handel, "Quantum approach to $1/f$ noise," *Phys. Rev.,* vol. 22A, p. 745, 1980.

[9] ——, "Fundamental quantum $1/f$ noise in semiconductor devices," *IEEE Trans. Electron Devices,* vol. 41, no. 11, pp. 2023–2033, Nov. 1994.

[10] ——, "Coherent and conventional quantum $1/f$ effect," *Phys. Status Solidi,* vol. b194, pp. 393–409, 1996.

[11] ——, "Noise, low frequency," in *Wiley Encyclopedia of Electrical and Electronics Engineering* J. G. Webster Ed. New York: Wiley, 1999, vol. 14, pp. 428–449.

[12] T. S. Sherif and P. H. Handel, "Unified treatment of diffraction and $1/f$ noise," *Phys. Rev.,* vol. A26, pp. 596–602, 1982.

[13] P. H. Handel and D. Wolf, "Characteristic functional of quantum $1/f$ noise," *Phys. Rev.,* vol. A26, pp. 3727–3730, 1982.

[14] F. N. Hooge, *Phys. Lett.,* vol. A-29, p. 139, 1969.

[15] G. S. Kousik, C. M. van Vliet, G. Bosman, and P. H. Handel, *Adv. Phys.,* vol. 34, pp. 663–726, 1985.

[16] G. S. Kousik, C. M. van Vliet, G. Bosman, and H.-J. Luo, *Phys. Status Solidi,* vol. 154, pp. 713–726, 1989.

[17] A. Van der Ziel, *Noise in Solid State Devices and Circuits*. New York: Wiley, 1986.

[18] ——, "Unified presentation of $1/f$ noise in electronic devices; fundamental $1/f$ noise sources," *Proc. IEEE,* vol. 76, no. 3, pp. 233–258, Mar. 1988.

[19] W. H. Press, *Comments Astrophys. Space Phys.,* vol. 7, p. 103, 1978.

[20] P. H. Handel, "The nature of fundamental $1/f$ noise," in *Proc. AIP Conf. 12th Int. Conf. Noise in Physical Systems and* $1/f$ *Fluctuations* 1993, vol. 285, pp. 162–171.

[21] ——, "$1/f$ noise—An infrared phenomenon," *Phys. Rev. Lett.,* vol. 34, pp. 1492–1494, 1975.

[22] ——, "The quantum $1/f$ effect and the general nature of $1/f$ noise," *Archiv fur Elektronik and Ubertragungstechnik (AEU),* vol. 43, pp. 261–270, 1989.

[23] A. van der Ziel, "Semiclassical derivation of Handel's expression for the Hooge parameter," *J. Appl. Phys.,* vol. 63, pp. 2456–2455, 1988.

[24] P. H. Handel, "Any particle represented by a coherent state exhibits $1/f$ noise," in *Proc. 7th Int. Conf. Noise in Physical Systems and* $1/f$ *Noise* M. Savelli, G. Lecoy, and J. P. Nougier Eds., 1983, p. 97.

[25] ——, "Coherent states quantum $1/f$ noise and the quantum $1/f$ effect," in *Proc. 8th Int. Conf. Noise in Physical Systems and* $1/f$ *Noise* A. D'Amico and P. Mazzetti Eds., 1986, p. 469.

[26] ——, "Incoherence and negative entropy in the quantum $1/f$ effect of BAW and SAW quartz resonators," in *Proc. 1997 IEEE Int. Frequency Control Symp.* J. R. Vig Ed., 1997, pp. 464–469.

[27] ——, *General Quantum* $1/f$ *Bibliography*. St. Louis, MO: Physics Dept., Univ. of Missouri.

[28] A. van der Ziel, "The experimental verification of Handel's expressions for the Hooge parameter," *Solid State Electron.,* vol. 31, pp. 1205–1209, 1988.

[29] A. van der Ziel, A. D. van Rheenen, and A. N. Birbas, "Extensions of Handel's $1/f$ noise equations and their semiclassical theory," *Phys. Rev.,* vol. B40, pp. 1806–1809, 1989.

[30] P. H. Handel, "Quantum $1/f$ quartz resonator theory versus experiment," in *Proc. 1999 Joint Eur. Frequency and Time Forum and IEEE Int. Frequency Control Symp.* 1999, pp. 1192–1195.

[31] A. Balandin, S. Cai, R. Li, K. L. Wang, V. Ramgopal Rao, and C. R. Viswanathan, "Flicker noise in GaN/$Al_{0.15}Ga_{0.85}N$ doped channel heterostructure field effect transistors," *IEEE Electron Device Lett.* vol. 19, no. 12, pp. 475–477–61, Dec. 1998.

[32] A. Balandin, K. L. Wang, R. Li, A. Svizhenko, and S. Bandyopadhyay, "The fundamental $1/f$ noise and the Hooge parameter in semiconductor quantum wires," *IEEE Trans. Electron Devices,* vol. 46, no. 6, pp. 1240–1244, Jun. 1999.

[33] M. Tacano, "Hooge fluctuation parameter of semiconductor microstructures," *IEEE Trans. Electron Devices,* vol. 40, no. 11, pp. 2060–2064, Nov. 1993.

[34] M. Tacano, A. Ando, I. Shibasaki, S. Hashiguchi, J. Sikula, and T. Matsui, "Dependence of Hooge parameter of compound semiconductors," in *Proc. AIP* P. H. Handel and A. L. Chung Eds., 1999, vol. 466, pp. 35–41.

[35] A. Balandin, K. L. Wang, A. Svizhenko, and S. Bandyopadadhyay, "The effects of low-dimensionality on the quantum $1/f$ noise," in *Proc. AIP* P. H. Handel and A. L. Chung Eds., 1999, vol. 466, pp. 131–134.

[36] A. Widom, V. Kidambi, and Y. N. Srivastava, "Soft boson radiation and fractal probability distributions," in *Proc. AIP* P. H. Handel and A. L. Chung Eds., 1999, vol. 466, pp. 135–144.

[37] J. Berntgen, T. L. Lim, W. Daumann, U. Auer, F.-J. Tegude, A. Matulionis, and K. Heime, "Hooge parameter of 2DEG structures and its dependence on channel design and temperature," in *Proc. AIP* P. H. Handel and A. L. Chung Eds., 1999, vol. 466, pp. 59–70.

[38] J. Berntgen, K. Heime, W. Daumann, U. Auer, F.-J. Tegude, and A. Matulionis, "The $1/f$ noise of InP based 2DEG devices and its dependence on mobility," *IEEE Trans. Electron Devices,* vol. 46, no. 1, pp. 194–203, Jan. 1999.

[39] J. Berntgen, A. Behres, J. Kluth, K. Heime, W. Daumann, U. Auer, and F. J. Tegude, "Hooge parameter of InGaAs bulk material and InGaAs 2DEG quantum well structures lattice matched to InP," in *Proc. 15th Int. Conf. Noise in Physical Systems and* $1/f$ *Fluctuations (ICNF'99)* C. Surya Ed., pp. 250–254.

[40] J. Berntgen, T. L. Lim, K. Heime, W. Daumann, U. Auer, F. J. Tegude, and A. Matulionis, "The Hooge parameter of 2DEG quantum well structures and its dependence on temperature," in *Proc. 15th Int. Conf. Noise in Physical Systems and* $1/f$ *Fluctuations (ICNF'99)* C. Surya Ed., pp. 291–299.

[41] M. Tacano, M. Ando, I. Shibasaki, S. Hashiguchi, J. Sikula, and T. Matsui, "Dependence of Hooge parameter of InAs heterostructure on temperature," in *Proc. 15th Int. Conf. Noise in Physical Systems and $1/f$ Fluctuations (ICNF'99)* C. Surya Ed., pp. 218–221.

[42] H. Ünlü, "Current transport and $1/f$ noise in heterojunction bipolar transistors," in *Proc. 15th Int. Conf. Noise in Physical Systems and $1/f$ Fluctuations (ICNF'99)* C. Surya Ed., pp. 295–299.

[43] S. Bandyopadhyay, A. Svizhenko, and M. A. Stroscio, "Electronic noise in quantum wires," *Phys. Low-Dim. Struct.,* vol. 3/4, pp. 1–242, 1999.

[44] P. H. Handel, "Instabilities, turbulence and flicker-noise in semiconductors I, II and III," *Zeitschrift für Naturforschung,* vol. 21a, pp. 561–593, 1966.

[45] ——, "Turbulence theory for the current carriers in solids and a theory of $1/f$ noise," *Phys. Rev.,* vol. A3, p. 2066, 1971.

[46] A. van der Ziel and P. H. Handel, "$1/f$ noise in n^+-p diodes," *IEEE Trans. Electron Devices,* vol. ED-32, no. 9, pp. 1802–1805, Sep. 1985.

[47] A. van der Ziel, P. H. Handel, X. L. Wu, and J. B. Anderson, "Review of the status of quantum $1/f$ noise in n^+-p HgCdTe photodetectors and other devices," *J. Vac. Sci. Technol.,* vol. A4, p. 2205, 1986.

[48] A. van der Ziel, P. Fang, L. He, X. L. Wu, A. D. van Rheenen, and P. H. Handel, "$1/f$ noise characterization of n^+-p and n-i-p $Hg_{1-x}Cd_xTe$ detectors," *J. Vac. Sci. Technol.,* vol. A 7, pp. 550–554, 1989.

[49] A. H. Pawlikiewicz, A. van der Ziel, G. S. Kousik, and C. M. Van Vliet, "Fundamental $1/f$ noise in silicon bipolar transistors," *Solid-State Electron.,* vol. 31, pp. 831–834, 1988.

[50] A. van der Ziel, C. J. Hsieh, P. H. Handel, C. M. Van Vliet, and G. Bosman, "Partition $1/f$ noise in pentodes and its quantum interpretation," *Physica,* vol. 145 B, pp. 195–204, 1987.

[51] A. van der Ziel, "Interpretation of Schwates's experimental data on secondary emission $1/f$ noise," *Physica,* vol. 144B, p. 205, 1986.

[52] P. Fang, L. He, A. D. Van Rheenen, A. van der Ziel, and Q. Peng, "Noise and lifetime measurements in Si p^+ power diodes," *Solid-State Electron.,* vol. 32, pp. 345–348, 1989.

[53] P. H. Handel and A. van der Ziel, "Relativistic correction of the Hooge parameter for Umklapp $1/f$ noise," *Physica,* vol. 141B, pp. 145–147, 1986.

[54] P. H. Handel, "Quantum $1/f$ noise in SQUIDs," in *Proc. 8th Int. Conf. Noise in Physical Systems 1985* A. D'Amico and P. Mazetti Eds., pp. 489–490.

[55] ***[AU: This reference is the same as [46]. Please provide correct reference.]***A. van der Ziel and P. H. Handel, "$1/f$ noise in n^+-p diodes," *IEEE Trans. Electron Devices,* vol. ED-32, pp. 1802–1805, 1985.

[56] J. R. Vig and F. L. Walls, "Fundamental limits on the frequency instabilities of quartz crystal oscillators," in *Proc. 48th Annu. Frequency Control Symp.* 1994, pp. 506–523.

[57] P. H. Handel, "Low frequency fluctuations in electronic transport phenomena," in *Proc. NATO Advanced Study Institute on Linear and Nonlinear Electronic Transport in Solids* J. T. Devreese and V. van Doren Eds., 1976, pp. 515–547.

[58] J. J. Gagnepain and J. Uebersfeld, "$1/f$ noise in quartz crystal resonators," in *Proc. 1st Symp. $1/f$ Fluctuations* T. Musha Ed., 1977, pp. 173–182.

[59] T. E. Parker, "$1/f$ frequency fluctuations in quartz acoustic resonators," in *Proc. 39th Annu. Frequency Control Symp.* 1985, pp. 97–106.

[60] P. H. Handel, "Second annual report," AFOSR Grant No. 89-0416, July 15, 1991, p. 8.

[61] F. L. Walls, P. H. Handel, R. Besson, and J. J. Gagnepain, "A new model relating resonator volume to $1/f$ noise in BAW quartz resonators," in *Proc. 46th Annu. Frequency Control Symp.* 1992, pp. 327–333.

[62] P. H. Handel, "Analysis of quantum $1/f$ effects in frequency standards," in *Proc. 46th Annu. Frequency Control Symp.* 1994, pp. 539–540.

[63] ——, "$1/f$ noise universality in high-technology applications," in *Proc. 1994 IEEE Int. Frequency Control Symp.* L. Maleki Ed., Boston, MA, pp. 8–21.

[64] J. R. Vig and Y. Kim, "Noise in microelectromechanical system resonators," *IEEE Trans. Ultrason., Ferroelectr., Freq. Control,* vol. 46, no. 6, pp. 1558–1565, Nov. 1999.

[65] C. T.-C. Nguyen, "Micromechanical resonators for oscillators and filters (invited)," in *Proc. 1995 IEEE Int. Ultrasonics Symp.* pp. 489–499.

[66] ——, "Micromachining technologies for miniaturized communication devices (invited plenary)," *Proc. SPIE, Micromachining and Microfabrication,* vol. 3515, pp. 24–38, 1998.

[67] ——, "Transceiver front-end architectures using vibrating micromechanical signal processors (invited)," in *Dig. Papers Topical Meeting Silicon Monolithic Integrated Circuits in RF Systems* 2001, pp. 23–32.

[68] ——, "Vibrating RF MEMS for low power wireless communications (invited keynote)," in *Proc. 2000 Int. MEMS Workshop (iMEMS'01)* pp. 21–34.

[69] S. Lee, M. U. Demirci, and C. T.-C. Nguyen, "A 10-MHz micromechanical resonator Pierce reference oscillator for communications," in *Dig. Tech. Papers 11th Int. Conf. Solid-State Sensors and Actuators (Transducers'01)* pp. 1094–1097.

[70] W.-T. Hsu, J. R. Clark, and C. T.-C. Nguyen, "Q-optimized lateral free-free beam micromechanical resonators," in *Dig. Tech. Papers 11th Int. Conf. Solid-State Sensors and Actuators (Transducers'01)* pp. 1110–1113.

[71] K. E. Sia, "The application of piezoelectric quantum $1/f$ noise theory to describe the low frequency noise in ELO-GaN and n-GaN," Ph.D. dissertation, Tech. Univ. Darmstadt, Darmstadt, Germany, 2003.

[72] E. S. Ferre-Pikal and F. L. Walls *et al.,* in *Proc. 50th Frequency Control Symp.* 1996, pp. 844–851.

[73] T. E. Parker and D. Andres, "$1/f$ noise in surface acoustic wave resonators," in *Proc. 48th Annu. Frequency Control Symp.* 1994, pp. 530–538.

[74] T. E. Parker, D. Andres, J. A. Greer, and G. T. Montress, "$1/f$ noise in etched groove surface acoustic wave resonators," *IEEE Trans. Ultrason., Ferroelectr., Freq. Control,* vol. 41, no. 6, pp. 853–862, Nov. 1994.

[75] P. H. Handel, H. L. Hartnagel, K. E. Sia, and D. Wolf, "Connection of coherent and conventional piezoelectric quantum $1/f$ noise and the role of subharmonics," in *Proc. 17th Int. Conf. Noise and Fluctuations (ICNF'03)* J. Sikula Ed., pp. 161–166.

[76] P. H. Handel, H. L. Hartnagel, K. E. Sia, U. K. Mishra, and R. York, "GaN HEMT geometry and piezoelectric quantum $1/f$ noise," in *Proc. WOCSDICE 2004* pp. 85–87.

[77] A. van der Ziel, "Generalized semiclassical quantum 1/f noise theory, I: Acceleration 1/f noise in semiconductors," *J. Appl. Phys.,* vol. 64, pp. 903–906, 1988.

[78] A. N. Birbas, Q. Peng, and A. van der ZielA. D. van Rheenen and K. Amberiadis, "Channel-length dependence of the $1/f$ noise in silicon metal-oxide-semiconductor field effect transistors, verification of the acceleration $1/f$ noise process," *J. Appl. Phys.,* vol. 64, pp. 907–912, 1988.

[79] T. E. Parker, "$1/f$ frequency fluctuations in quartz acoustic resonators," *Appl. Phys. Lett.,* vol. 46, no. 3, pp. 246–248, Feb. 1, 1985.

Peter H. Handel, (Senior Member, IEEE) received the M.S. degree in atomic and theoretical physics and the Ph.D. degree in solid-state theory in 1965, both from the University of Bucharest, Bucharest, Romania.

From 1960 to 1967, he was a Scientist at the Institute of Physics of the Romanian Academy, Bucharest. During 1967–1969, he was a Scientist at the Max V. Laue Paul Langevin Institute, Munich, Germany. He has been a Professor of Physics at the University of Missouri, St. Louis, since 1969. He developed the quantum theory of $1/f$ noise in 1975 and researched the infrared divergence effect of $1/f$ fluctuations in physical cross sections and process rates. In 1981, he developed a polarization catastrophe theory of atmospheric electricity. He has also made contributions to solid-state, plasma, and electronic noise theory. The simple coherent and conventional quantum $1/f$ effect formulas are applicable to most high-technology materials, systems, and devices, particularly useful in nanotechnology.

Dr. Handel has been organizer and Chairman of the Quantum $1/f$ Symposia since 1990. He is also a member of the Center for Molecular Electronics of the University of Missouri at St. Louis. Since 2001, he has also been a Member of the ultralow phase noise Multidisciplinary Research Initiative at the University of California, Santa Barbara.

Adam G. Tournier received the B.A. degree in physics and the M.S. degree in atomic physics from the University of Missouri, St. Louis, in 2000 and 2002, respectively. He is currently working toward the Ph.D. degree at the University of Missouri, Rolla.

In 2003 and 2005 he was a research assistant with P. H. Handel working on $1/f$ noise and the resulting $1/f3$ phase noise in resonators, oscillators, and resonant sensors.